BIOPROBES 58

CELL BIOLOGY BY INVITROGEN

APRIL 2009

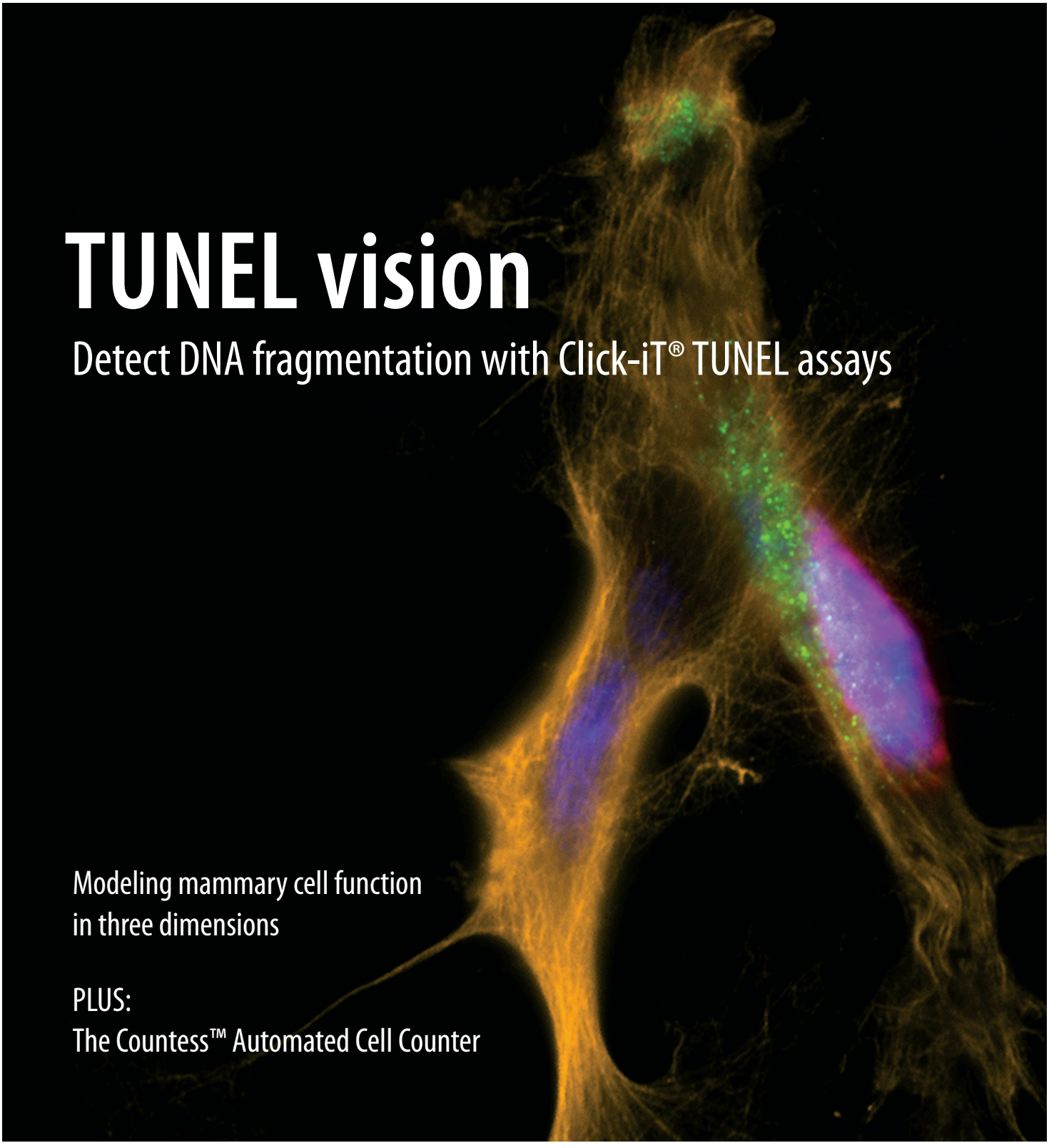

TUNEL vision

Detect DNA fragmentation with Click-iT® TUNEL assays

Modeling mammary cell function in three dimensions

PLUS:
The Countess™ Automated Cell Counter

invitrogen™

MOLECULAR PROBES®

MAKE THE MOST OF EVERY CELL

BioProbes® newsletter is published several times each year. *BioProbes* is dedicated to furnishing researchers with the very latest information about cell biology products and their applications. For a listing of our products, along with extensive descriptions and literature references, please see our website. Prices are subject to change without notice. Quantity discounts may be available.

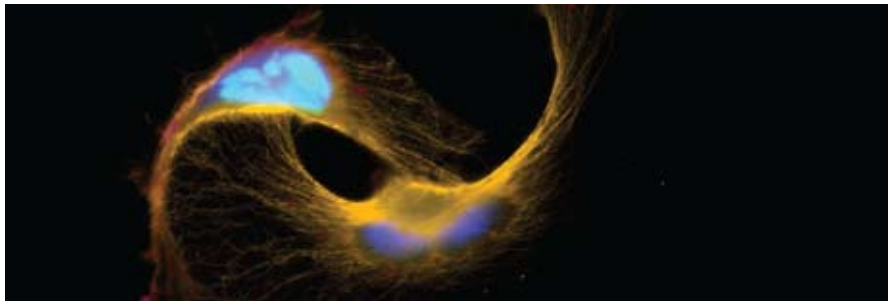

BioProbes 58

bioprobes@invitrogen.com

2008 APEX® AWARDS FOR PUBLICATION EXCELLENCE

Features

Departments

invitrogen™

Staining DNA without altering its structure

Wojcik, K. and Dobrucki, J.W. (2008) Interaction of a DNA intercalator DRAQ5, and a minor groove binder SYTO17, with chromatin in live cells—influence on chromatin organization and histone–DNA interactions. *Cytometry* 73A:555–562.

Do DNA-binding dyes alter the structure of their target? Nucleic acid–binding dyes are widely employed to provide information about the local concentration and distribution of DNA in the nuclei of living cells. However, binding of certain dyes may actually induce structural changes in chromatin, a sort of biological "observer effect" that could compromise our understanding of chromatin's *in vivo* organization.

To investigate the impact of dye binding on native chromatin structure, Wojcik and Dobrucki examined changes in the chromatin of HeLa cells expressing eGFP-tagged linker (H1) and core (H2B) histones. Binding of DRAQ5—a DNA intercalator—was observed to be accompanied by chromatin aggregation, even in the presence of as little as 1 µM dye; the authors suggest that structural changes beyond the resolution of optical microscopy likely begin even at submicromolar dye concentrations. Increasing the dye concentration to 3 µM led to further aggregation and gradual loss of chromatin organization; 7.5 µM DRAQ5 was sufficient to randomize the chromatin distribution to the point where heterochromatin and euchromatin were no longer discernible. Fluorescence microscopy also revealed the detachment of H1 and (to a lesser degree) H2B histones as a result of DRAQ5 binding. Similar effects were observed when DRAQ5 dye was replaced by the intercalating drugs adriamycin and daunomycin. In line with the reported role of histone H1 as a principal stabilizing factor for chromatin structure, the authors suggest a "self-promoting" mechanism in which intercalation leads to histone H1 detachment, which exposes new stretches of DNA for further intercalation and destabilization.

The team then examined the effect of Molecular Probes® SYTO® 17 dye—a minor-groove binder—on chromatin structure. At concentrations of SYTO® 17 dye up to 7.5 µM, only slight aggregation of chromatin was observed; no histone detachment was detected over the experimental concentration range. Based on their observations, the authors describe the impact of SYTO® 17 dye binding on chromatin structure as "negligible", a potentially highly relevant conclusion for researchers conducting sensitive live-cell imaging experiments. The authors suggest that the observed loss of chromatin structure upon intercalator binding may be relevant in flow cytometry assays that use DNA-binding dyes in live cells, and could provide important structural insight in future studies of the mechanism of drugs known to act through DNA intercalation.

To learn more about SYTO® dyes for nucleic acid staining, visit **www.invitrogen.com**. ■

Product	Quantity	Cat. no.
SYTO® 17 red fluorescent nucleic acid stain, 5 mM solution in DMSO	250 µl	S7579

BioSource™, Caltag™, and Zymed® products now bear the core Invitrogen brand

MAKE THE MOST OF EVERY CELL WITH INVITROGEN CELL BIOLOGY: NOW ISO 13485 CERTIFIED

Beginning October 15, 2008, the mix of products that you recognized as BioSource™, Caltag™, and Zymed® began carrying the Invitrogen brand. These products will continue to be manufactured using the same high-quality processes and specifications, and are now manufactured under ISO 13485 certification.

Invitrogen continues to deliver world-class tools for cell biology—our consolidation of BioSource™, Caltag™, and Zymed® means better service for you. You'll get the same trusted, high-quality products and technologies, fortified by Invitrogen's world-class sales, distribution, and product support structure.

If you have any questions, please contact your Invitrogen Sales Representative or email our Technical Support department at **support@invitrogen.com**.

Easy access to Molecular Probes® products

Finding the Molecular Probes® products you need has never been easier. At the new Molecular Probes® web page (**www.invitrogen.com/probes**), everything you need to find the right fluorescent products for your research is at your fingertips. You'll have quick access to key pages and resources, including:

- The online version of the Molecular Probes® *Handbook*, your premier source for technical information about Molecular Probes® products and their applications, including references and technical application notes (**www.invitrogen.com/handbook**)
- The Molecular Probes® products page, where you'll find more information about key Molecular Probes® products, including the Alexa Fluor® dyes, Qdot® nanocrystals, Click-iT® EdU cell proliferation assays, and much more (**www.invitrogen.com/probesproducts**)
- Resources like the Fluorescence SpectraViewer, our fluorescence and flow cytometry tutorials, the K_d calculator, and the Molecular Probes® Image Gallery

Visit **www.invitrogen.com/probes** today for easy access to Molecular Probes® products and resources. ■

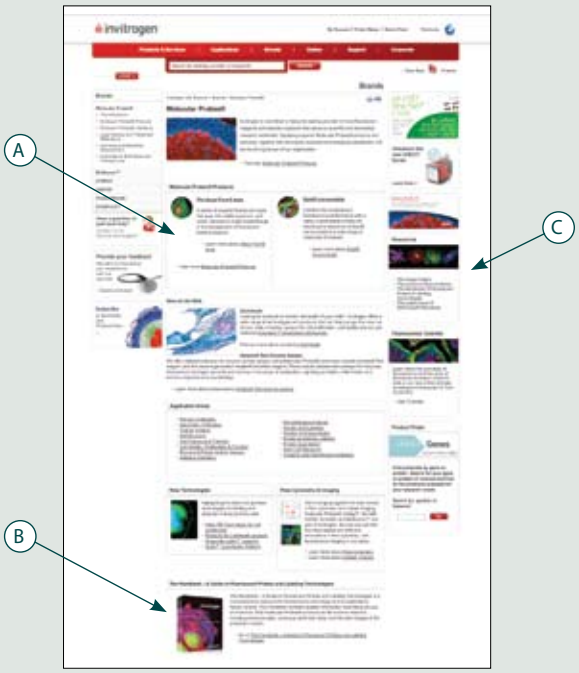

The Molecular Probes® brand page.

A. *The Molecular Probes® products page.*

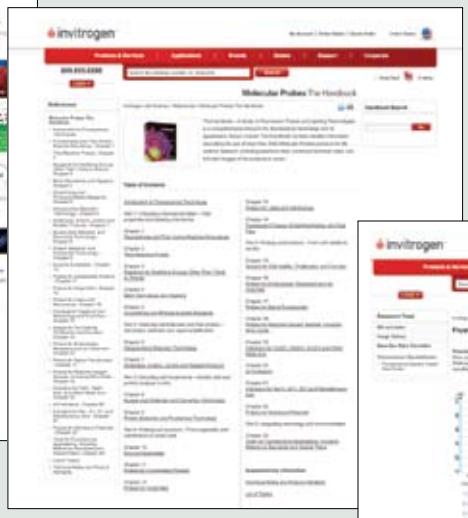

B. The *Molecular Probes®* Handbook.

C. *The Molecular Probes® Fluorescence SpectraViewer.*

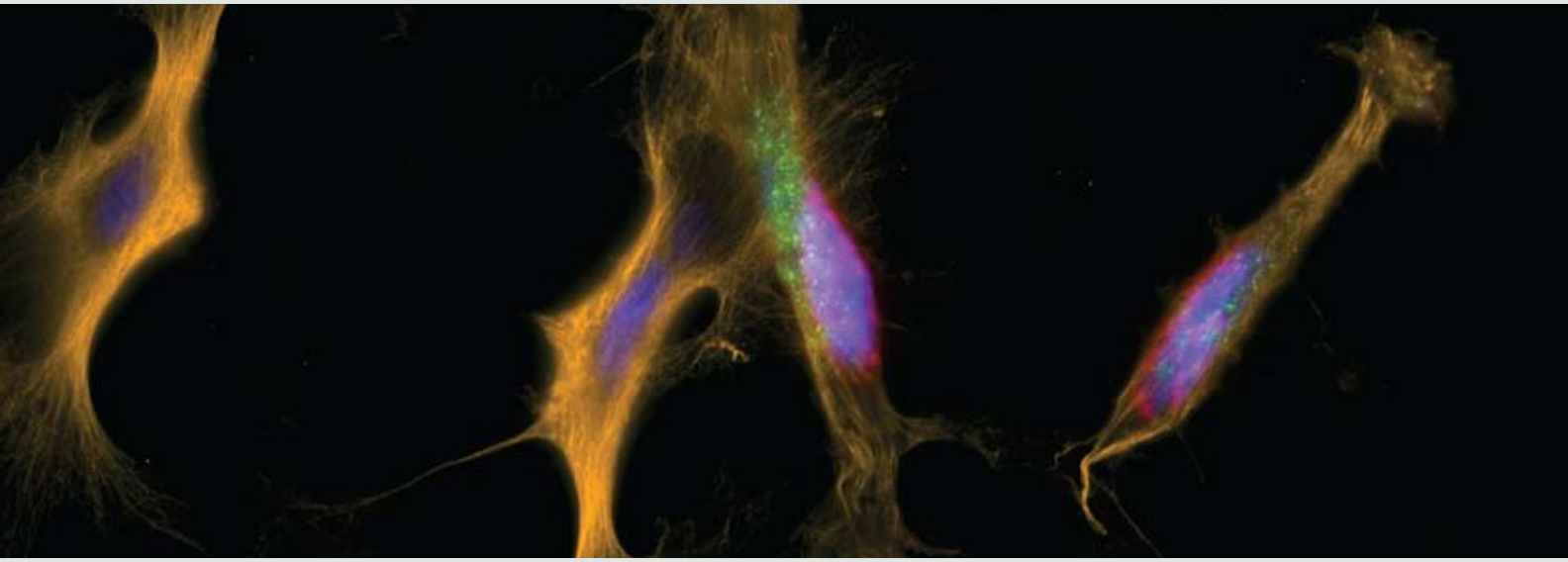

TUNEL vision

DETECT DNA FRAGMENTATION WITH CLICK-IT® TUNEL ASSAYS.

At the final stage of apoptosis, adherent cells often detach from the slide or well before they can be detected. Because cells are lost in this way, you may not be able to detect the DNA fragmentation that is a hallmark, as well as the ultimate determinant, of apoptosis.[1] Since its introduction in 1992,[2] the most widely used *in situ* test for studying DNA fragmentation or strand breaks is the terminal deoxynucleotidyl transferase-dUTP nick end labeling (TUNEL) assay, which is based on the incorporation of modified dUTPs by terminal deoxynucleotidyl transferase (TdT) at the 3´-OH ends of fragmented DNA. For a reliable and reproducible TUNEL imaging assay, it is vital not only that the modified nucleotide is an acceptable substrate for TdT, but also that the detection method is sensitive and avoids any additional loss of cells from the sample. The Click-iT® TUNEL Imaging Assays meet both of these criteria. The alkyne-modified dUTP used in the Click-iT® TUNEL assay is rapidly incorporated by TdT, providing sensitive detection that allows you to fix your samples earlier and preserve late-stage apoptotic cells for imaging before they can detach (Figure 1). Compared with assays that use other modified nucleotides, the fast and reliable Click-iT® TUNEL Imaging Assays can detect a higher percentage of apoptotic cells under identical conditions in much less time.

Figure 1 (above)—DNA strand breaks typical of late-stage apoptosis visualized using the Click-iT® TUNEL Imaging Assay. HeLa cells were treated with staurosporine, then fixed and permeabilized. The Click-iT® TUNEL Alexa Fluor® 647 Imaging Assay (Cat. no. C10247) was performed. Activated caspase-3 was detected with a rabbit polyclonal primary antibody for cleaved caspase-3 and labeled with Alexa Fluor® 488 goat anti–rabbit IgG (Cat. no. A11008, green fluorescence). Tubulin was detected with a mouse monoclonal anti-tubulin antibody and labeled with Alexa Fluor® 555 goat anti–mouse IgG (Cat. no. A21422, orange fluorescence). Nuclei were stained with Hoechst 33342 (Cat. no. H1399, blue fluorescence). The coverslips were mounted in ProLong® Gold antifade reagent (Cat. no. P36930) before imaging. The cells on the right not only have a high level of caspase-3 activity and DNA strand breaks, but also show a loss of structural integrity consistent with cells undergoing apoptosis.

Detect late-stage apoptosis before cells "pop"

The Click-iT® TUNEL Imaging Assays use a dUTP modified with an alkyne, a small, bio-orthogonal functional group that allows the nucleotide to be more readily incorporated by TdT than other modified nucleotides are (Figures 2 and 3). The enzymatically incorporated nucleotide is detected with a click reaction—a copper-catalyzed triazole formation between an azide and an alkyne (Figure 4). Click reactions have several characteristics: the reaction between the detection moieties is efficient; no extreme temperatures or solvents are required; the reaction product is stable; and the components of the reaction are bioinert, which means that no side reactions occur—the label and the detection tags react selectively with one another.[3–6] This final point is the greatest advantage of this powerful detection technique; click chemistry–labeled molecules can be applied to complex biological samples and detected with unprecedented sensitivity, thanks →

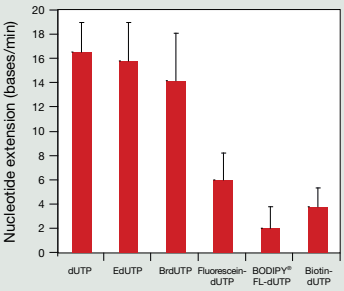

Figure 3—Comparison of TdT incorporation of several modified nucleotides. A 48-base single-strand DNA primer plus one type of dUTP nucleotide were incubated with 30 units of TdT enzyme for 3 hr at 37°C. The reaction mixtures were applied to a 20% TBE gel. The gel was stained with ethidium bromide and imaged on a FLA 9000 Fuji scanner. The length of the primer extension was measured by comparing it to the standard 25 bp DNA ladder. To calculate the number of dUTPs added per minute, the length in nucleotides was divided by the time of incubation.

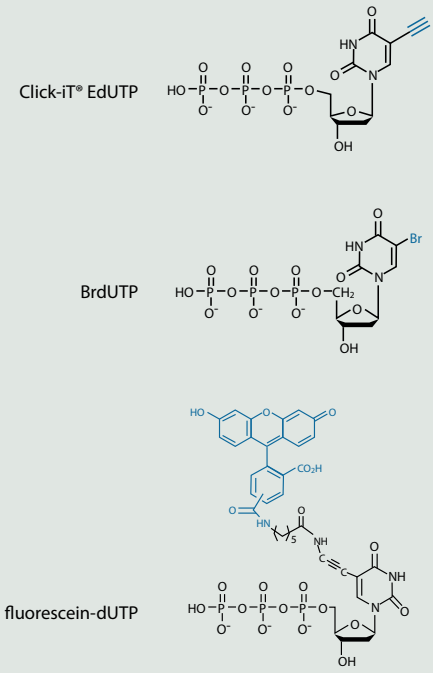

Figure 2—Modified nucleotide structures. The alkyne and bromine modifications are significantly smaller than fluorescein.

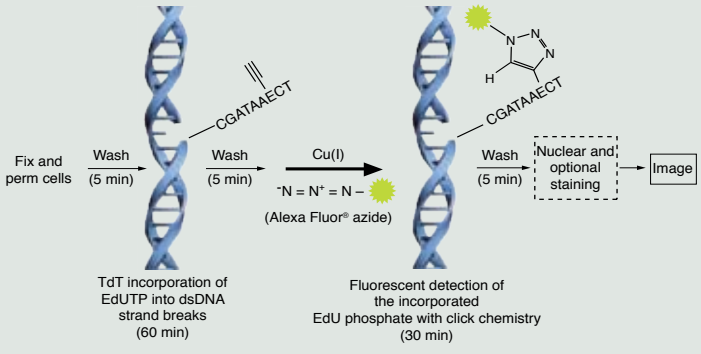

Figure 4—Detection of apoptosis with the Click-iT® TUNEL assay.

to extremely low background. As a result, when compared with assays using one of the other modified nucleotides, the Click-iT® TUNEL assay is able to detect a higher percentage of apoptotic cells under identical conditions (Figure 5) within 2 hours.

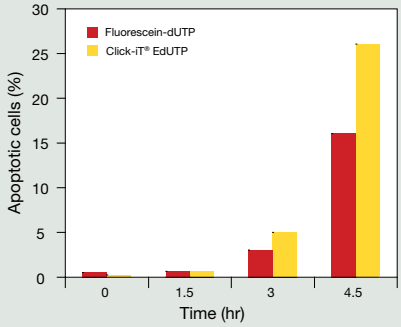

Figure 5—TUNEL assay time course comparison showing the percentage of apoptotic cells detected. HeLa cells were treated with 0.5 µM staurosporine for the lengths of time indicated. Following fixation and permeabilization, TUNEL assays using either Click-iT® EdUTP or fluorescein dUTP (DeadEnd™ Colorimetric TUNEL System, Promega) were performed according to the manufacturer's instructions. The percentage of apoptotic cells was calculated based upon the corresponding negative control. Imaging and analysis was performed using a Thermo Scientific Cellomics® ArrayScan® II (Thermo Fisher Scientific).

Straightforward multiplexed analyses of programmed cell death

To unequivocally establish programmed cell death in any given cell or tissue model, two or more biomarkers of apoptosis must be multiplexed. The Click-iT® TUNEL Imaging Assays are available with a choice of several bright and photostable Alexa Fluor® dyes, ranging from green to far-red fluorescence, providing unprecedented flexibility when working with other apoptosis detection reagents that may only be available in green- or red-fluorescent options. The Click-iT® TUNEL assays have been tested in HeLa, A549, and CHO K1 cells with a variety of reagents that induce apoptosis, including staurosporine, and multiplexed with antibody-based detection of other apoptosis biomarkers such as cleaved poly(ADP-ribose) polymerase (PARP), cleaved caspase-3, or phosphohistone 2B (Figure 6). Each Click-iT® TUNEL kit contains all of the components necessary to accurately and reliably detect DNA fragmentation in adherent cells grown on coverslips or in 96-well microplates. Learn more at **www.invitrogen.com/click**. ■

References

1. Gavrieli, Y. et al. (1992) *J Cell Biol* 119:493–501.
2. Huerta, S. et al. (2007) *J Surg Res* 139:143–156.
3. Breinbauer, R. and Köhn, M. (2003) *Chembiochem* 4:1147–1149.
4. Wang, Q. et al. (2003) *J Am Chem Soc* 125:3192–3193.
5. Rostovtsev, V.V. et al. (2002) *Angew Chem Int Ed Engl* 41:2596–2599.
6. Kolb, H.C. et al. (2001) *Angew Chem Int Ed Engl* 40:2004–2021.

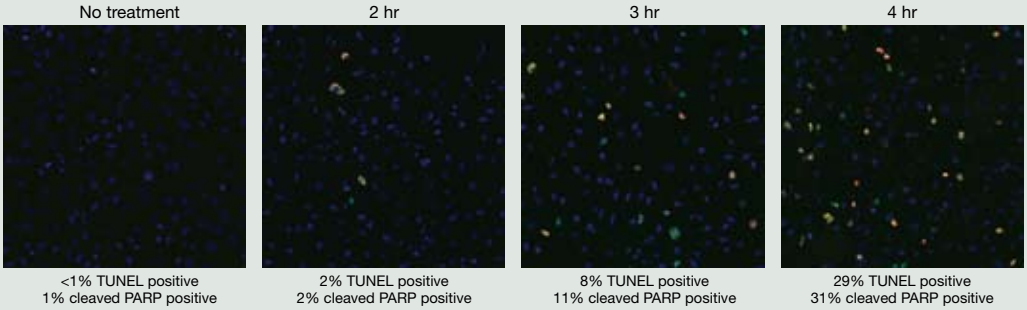

Figure 6—Click-iT® TUNEL assays used with antibody-based apoptosis detection. HeLa cells were treated with 0.5 µM staurosporine for the lengths of time indicated. The cells were fixed and permeabilized, followed by treatment with the Click-iT® TUNEL Alexa Fluor® 594 Imaging Assay (Cat. no. C10246). Cleaved PARP was detected with a rabbit anti–cleaved PARP antibody and visualized using an Alexa Fluor® 488 goat anti–rabbit IgG antibody (Cat. no. A11034). Cells exhibiting yellow fluorescence are positive for both cleaved PARP (green fluorescence) and DNA strand breaks (red fluorescence). The images were quantitated using the Thermo Scientific Cellomics® ArrayScan® VTI platform (Thermo Fisher Scientific).

Product	Quantity	Cat. no.
Click-iT® TUNEL Alexa Fluor® 488 Imaging Assay for microscopy and HCS, 50–100 assays	1 kit	C10245
Click-iT® TUNEL Alexa Fluor® 594 Imaging Assay for microscopy and HCS, 50–100 assays	1 kit	C10246
Click-iT® TUNEL Alexa Fluor® 647 Imaging Assay for microscopy and HCS, 50–100 assays	1 kit	C10247

Assess hERG channel blocks without radioactivity

THE PREDICTOR™ hERG FLUORESCENCE POLARIZATION ASSAY KIT.

Potentially cardiotoxic off-target effects of compounds at the human ether-a-go-go related gene (hERG) potassium channel continue to challenge the development of effective and safe pharmaceuticals. hERG channel function is critical to ventricular repolarization, and compounds that block the channel can produce a heart rhythm disorder known as long QT syndrome,[1,2] characterized by an increased duration between the QRS complex and T wave of a body surface electrocardiogram. This compromised cardiac repolarization can result in a characteristic arrhythmia known as torsades de pointes, which may either revert to normal sinus rhythm or degenerate into ventricular fibrillation and lead to sudden death.[2]

Patch-clamp electrophysiology is the most accurate functional measure of the interactions a compound might have with the hERG channel, but the cost of these assays prevents routine implementation at the early stages of discovery. Instead, radioligand displacement assays have been used routinely as an initial screen because many compounds that block the hERG channel interact at a common site in the inner vestibule of the channel, primarily with two aromatic residues.[1,2] Still, using and disposing of radioligands is an unattractive option, and throughput suffers from their inherently heterogeneous nature. We have developed the Predictor™ hERG fluorescence polarization assay [3] to provide a homogeneous, high-throughput solution to determine compound affinity for the hERG channel (Figure 1).

The Predictor™ hERG fluorescence polarization assay

The Predictor™ assay requires only the simple addition of 4X test compounds, 2X Predictor™ hERG Membranes, and 4X Predictor™ hERG Tracer Red. Plates are incubated for 1–3 hours before measuring fluorescence polarization on a plate reader using excitation at 530 nm and emission at 585 nm. The Predictor™ assay kit provides an optimized protocol and reagent set that tolerate the presence of multiple solvents (>5% DMSO, EtOH, MeOH), provide stable reads for up to 24 hours on multiple instrument platforms, and can be used manually or with automated systems. Lot-to-lot reproducibility and quality control ensure consistent assay windows of >100 mP and Z´-factor of >0.5.

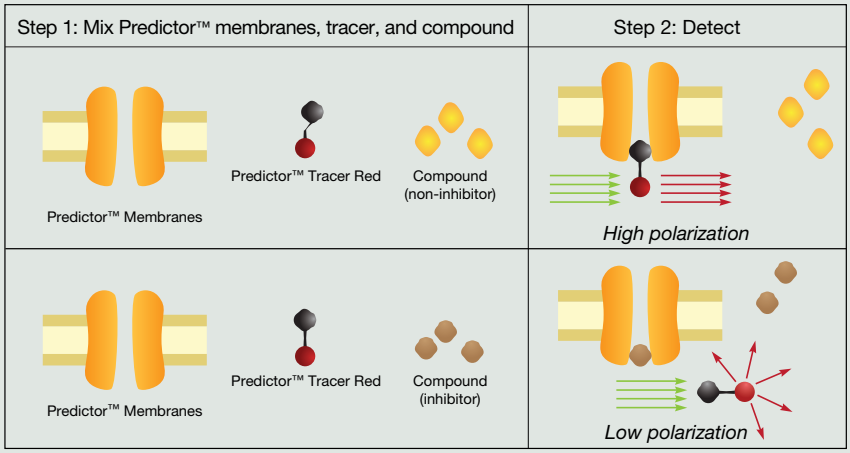

Figure 1—Predictor™ hERG fluorescence polarization assay principle. Fluorescence polarization is based on the observation that when a small fluorescent molecule (the tracer) is excited with plane-polarized light, the emitted light becomes depolarized because the molecule tumbles rapidly in solution during its fluorescent lifetime. If the tracer is bound to a large molecule, the tracer's rotation is slowed and the light remains highly polarized.

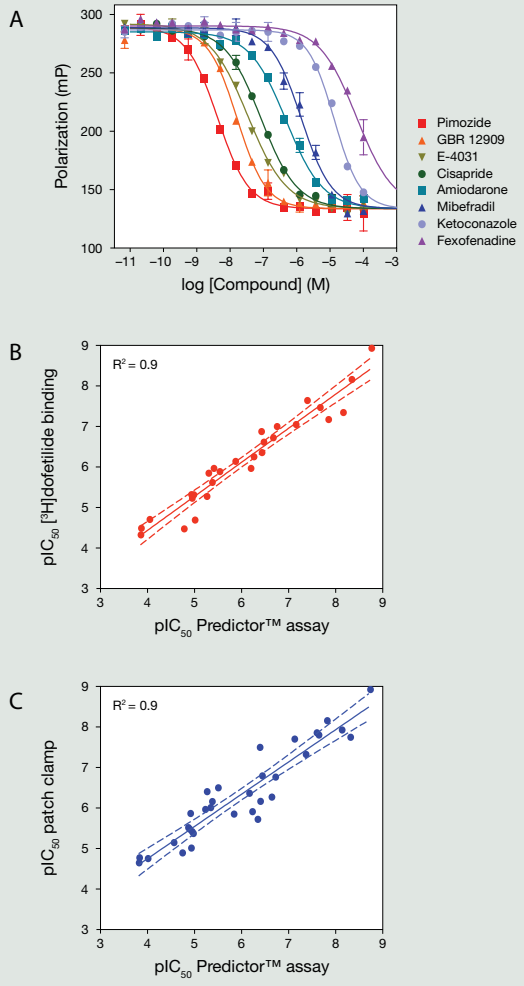

D

Compound	Assay-specific IC_{50} (mM)			
	Radioligand binding		Predictor™ assay	Patch clamp
	[^{3}H]Astemizole	[^{3}H]Dofetilide		
Astemizole	0.00	0.00	0.00	0.00
Pimozide	0.02	0.01	0.00	0.02
E-4031	0.08	0.02	0.04	0.05
Terfenadine	0.13	0.03	0.02	0.02
Dofetilide	0.04	0.04	0.01	0.01
GBR 12909		0.06	0.01	0.01
Cisapride	0.16	0.08	0.07	0.02
Haloperidol	0.30	0.09	0.17	0.17
Droperidol		0.12	0.37	0.03
Bepridil	0.78	0.17	0.21	0.55
Domperidone		0.22	0.33	0.16
Amiodarone	0.75	0.40	0.36	0.70
Thioridazine	1.14	0.51	0.54	1.25
Mibefradil		0.66	1.32	1.43
Verapamil	4.94	0.99	3.80	0.71
Propafenone		1.00	0.62	0.44
Clozapine		1.20	2.83	0.32
Quinidine	13.16	1.31	4.88	0.40
Fluoxetine	11.99	2.23	4.08	0.99
Imipramine	14.06	4.48	11.38	3.40
Flecainide	38.49	4.54	10.09	3.91
Pyrilamine		5.00	5.32	1.10
Desipramine		5.53	10.96	1.39
Sparfloxacin		18.80	86.61	18.00
Ketoconazole	19.05	19.50	9.48	4.36
Diltiazem		31.20	131.0	17.30
Fexofenadine	166.7	32.00	16.13	13.10
Spironolactone		45.70	134.5	23.00
Grepafloxacin		68.90	>500	50.00
Erythromycin	328.5	89.20	>500	152.7
Nifedipine			>500	>50
Glyburide	318.5		>500	74.00
Sertindole			0.02	0.01
Flunarizine			0.41	1.95
Tamoxifen	0.91		1.13	
Amitriptyline	15.55		10.53	10.00
Maprotiline			12.17	3.10
Papaverine			24.51	7.30
Mean fold change	0.46	1.82		3.31
Standard deviation	0.27	1.23		3.21
n	19	28		33

Figure 2—Pharmacology of the Predictor™ hERG fluorescence polarization assay. (**A**) The Predictor™ assay was used to generate IC_{50} data for 38 known hERG channel blockers from duplicate wells. Eight examples are shown (mean ± SEM; n = 2). Some curve fits were constrained to the minimum polarization produced by 30 µM E-4031. The IC_{50} values are tightly correlated to radioligand binding (**B**) and patch-clamp data (**C**) with a slope near unity. The 95% confidence intervals of the fit are shown as dashed lines. Pearson's correlation coefficient $R^2 = 0.9$ for both. (**D**) Comparison of data generated by the Predictor™ assay to radioligand binding and patch-clamp recordings reported or summarized in the literature.[4] Mean fold change is relative to Predictor™ data.

Performance and partial automation of the Predictor™ assay

While easily manipulated by hand, the assay can also be transferred to automated equipment. A set of 38 known hERG channel blockers that represent a wide range of structural space and chemical affinity was tested in such a fashion (Figure 2). Test compounds (5 µl at 4X) were dispensed to a 384-well plate (Corning, #3677) using a Biomek® FX Laboratory Automation Workstation (Beckman Coulter, Inc.). The Biomek® FX workstation was then used to dispense 10 µl of 2X Predictor™ hERG Membranes, followed by 5 µl of 4X Predictor™ hERG Tracer Red. Each compound was tested in the absence and presence of 30 µM E-4031 to correct for test compound interference as suggested by the Predictor™ protocol. Plates were incubated for 4 hours before measuring fluorescence polarization on a Safire^{2}™ microplate reader (Tecan) using excitation at 530 nm and emission at 585 nm (20 nm bandwidth). Using this automated technique, the Predictor™ assay identified IC_{50} values that were tightly correlated to and within a narrow range of the published values determined by radioligand binding assays and patch-clamp recordings.

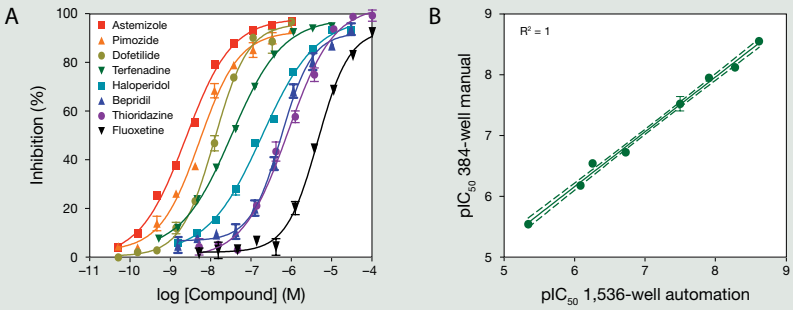

C

Compound	IC_{50} (nM) Automated 1,536-well	IC_{50} (nM) Manual 384-well (n = 3)
Astemizole	2.4	2.8 ± 0.46
Pimozide	5.2	7.5 ± 0.76
Dofetilide	12.2	11 ± 2
Terfenadine	31.3	30 ± 7
Haloperidol	185	189 ± 28
Bepridil	552	285 ± 33
Thioridazine	811	656 ± 41
Fluoxetine	4470	2862 ± 195

Figure 3—Successful 1,536-well automation of the Predictor™ hERG fluorescence polarization assay. The assay was automated to generate IC_{50} data for 8 known hERG channel blockers (**A**; values shown are means ± SEM for 4 wells). Data generated by the manual Predictor™ assay in 384-well format (three separate experiments) were compared to data generated on automation in 1,536-well format (**B, C**). The IC_{50} values were tightly correlated with a slope near unity and a Pearson's correlation coefficient $R^2 = 1$. The 95% confidence intervals of the fit are shown as dashed lines.

Miniaturization and complete automation of the Predictor™ assay

The throughput of the Predictor™ assay was further tested by miniaturizing to 1,536-well microplates and automating the dilution of the compound set (Figure 3). Compounds (80 nl, 100% DMSO) were dispensed to the assay plate with an Echo® 550 liquid handler (LabCyte).

Predictor™ hERG Membranes (4 µl) were dispensed to the assay plate with a Biomek® FX workstation. Predictor™ hERG Tracer Red (2 µl) and assay buffer (1.92 µl, with or without 30 µM E-4031) were dispensed to the assay plate with a CyBi®-Drop 3D dispenser (CyBio). Each compound was tested in the absence and presence of 30 µM E-4031, and plates were incubated for 4 hours before measuring fluorescence. The data generated from this automated and miniaturized technique were compared to those generated by hand on three separate occasions. The two methods were essentially indistinguishable and demonstrate the ease-of-use and robustness of the assay with respect to reagent dispensation and plate format.

Screening service

Rapidly assess hERG channel blocks with the SelectScreen® hERG Screening Service. This service uses the Predictor™ hERG Fluorescence Polarization Assay Kit to quickly identify compounds that bind the hERG channel, without the use of radioligands or the high cost of patch-clamp experiments. The SelectScreen™ hERG Screening Service offers high-quality data, 10-point dose response curves in duplicate, a guaranteed two-week turnaround time, and controls on every plate. To learn more, contact **discoveryservices@invitrogen.com**.

Improved early assessment of hERG liability

The Predictor™ hERG Fluorescence Polarization Assay Kit was developed to provide a safe, robust, reliable, stable, and high-throughput solution for determining the affinity of compounds for the hERG ion channel that is highly correlated to patch-clamp–determined compound pharmacology. Coupled with its ability to be integrated into automation workflows and miniaturized to a 1,536-well format, these added values far exceed the capabilities of radioligand displacement assays and result in a greater ability to assess hERG liability earlier in the discovery process. Learn more about this assay at **www.invitrogen.com/bp58**. ■

References

1. Mitcheson, J.S. et al. (2000) *Proc Natl Acad Sci U S A* 97:12329–12333.
2. Fernandez, D. et al. (2004) *J Biol Chem* 279:10120–10127.
3. Piper, D.R. et al. (2008) *Assay Drug Dev Technol* 6:213–223.
4. Diaz, G.J. et al. (2004) *J Pharmacol Toxicol Methods* 50:187–199.

Product	Quantity	Cat. no.
Predictor™ hERG Fluorescence Polarization Assay Kit	1 kit	PV5365
Each kit contains sufficient reagents for 400 wells in 384-well format.		

Characterization of type II kinase inhibitors and nonactivated kinases

THE LANTHASCREEN® EU KINASE BINDING ASSAY.

Traditional high-throughput screening (HTS)-compatible kinase activity assays have contributed to an increase in the number of kinase inhibitors reaching clinical trials, especially for applications in oncology. However, activity-based assays can have limitations in their breadth of target coverage or in the type of information they provide. Because activity assays measure a signal that is dependent on an active kinase, they are not well suited to characterize compounds that bind preferentially to the low-activity (nonactivated) form of a kinase, as is the case for type II kinase inhibitors such as Gleevec® (Novartis).[1] Additionally, compound on- or off-rates can be cumbersome to assess in an activity assay; measuring compound binding rather than kinase activity can overcome this limitation.

A broad kinase assay platform based on inhibitor binding

Invitrogen has developed a kinase assay platform based on measuring the binding and displacement of an Alexa Fluor® 647 conjugate of an ATP-competitive kinase inhibitor (tracer) at a kinase active site. Binding of the tracer to the kinase is detected by addition of a europium (Eu)-labeled antibody that recognizes a convenient protein tag, such as GST or His, which specifically labels the kinase of interest. This binding results in a high degree of fluorescence resonance energy transfer (FRET), whereas displacement of the tracer with a kinase inhibitor results in a loss of FRET (Figure 1). Using a small set of broad-spectrum kinase tracers, a Eu–anti-GST antibody, and a highly improved Eu–anti-His antibody, we have established assay conditions and validated the LanthaScreen® Eu kinase binding assay for more than 180 of the 300

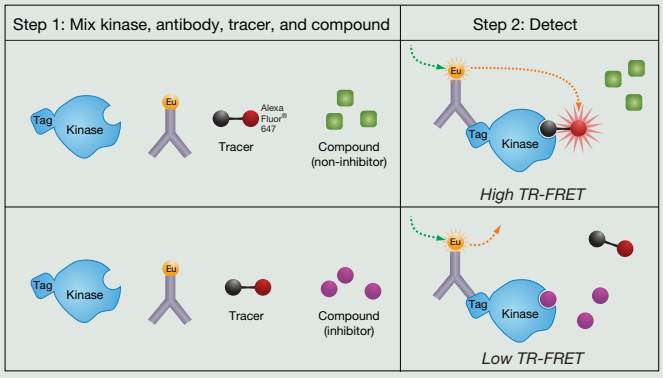

Figure 1—Schematic of the LanthaScreen® Eu kinase binding assay. The FRET signal is dependent on the specific binding of a Eu–anti-tag antibody to the tagged kinase of interest, ensuring that no signal arises due to any other enzymes in the test sample.

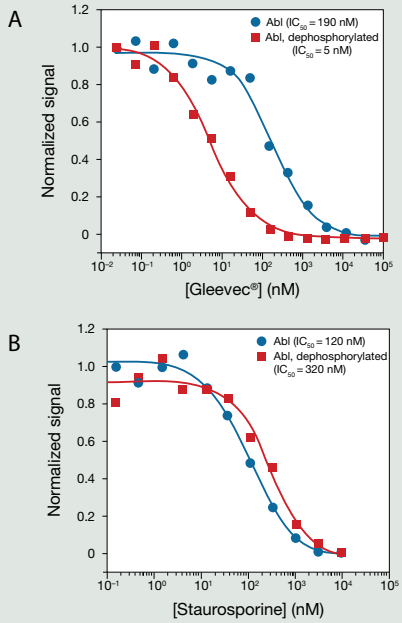

Figure 2—Preferential binding of the type II inhibitor Gleevec® to dephosphorylated Abl. (**A**) The affinity of Gleevec® was measured using the binding assay by mixing His-tagged Abl, with and without phosphatase treatment, with Kinase Tracer 236 and Eu–anti-His-Tag antibody, followed by TR-FRET measurement. (**B**) Staurosporine (an inhibitor that binds the active site) showed similar affinity for the active and the dephosphorylated kinase, in contrast to Gleevec®.

kinases in the Invitrogen™ portfolio. This broad coverage includes several kinases for which high-throughput activity assays have been difficult to develop. A current list of kinases for which the assay has been validated can be found on our website.

Assays of nonactivated kinases using type II kinase inhibitors

Using time-resolved FRET (TR-FRET), the LanthaScreen® Eu kinase binding assay has been used to demonstrate tight binding of Gleevec® to the dephosphorylated kinase Abl and weaker binding to active (phosphorylated) Abl (Figure 2). Gleevec® bound phosphatase-treated Abl with nearly 40-fold higher affinity than untreated Abl; the affinity of the control compound staurosporine was similar for the two forms.

Discrimination of kinase activity of interest

A challenge often faced when developing kinase activity assays, especially for less-studied targets and those with low specific activity, is ensuring that the measured activity is due to the target of interest, not low levels of contaminating kinases. This is particularly true when using generic substrates and when specific control inhibitors are unavailable. The LanthaScreen® Eu kinase binding assay has proven to be a viable solution for these types of targets, enabling validated assays for more than 30 kinases lacking robust activity assays, including DDR1, CDK8, and TGFBR1 (ALK5).

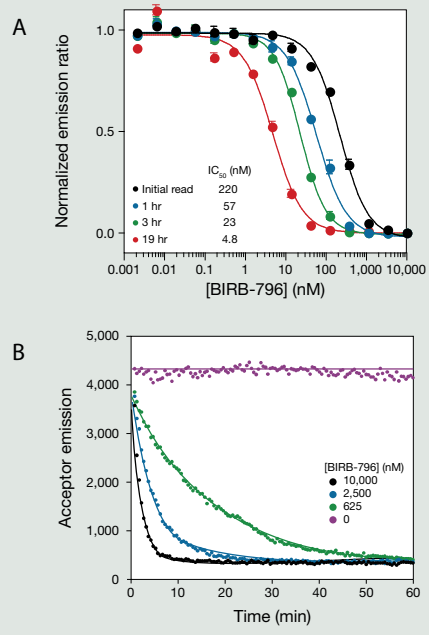

Figure 3—Slow binding of the type II kinase inhibitor BIRB-796 to p38α. (**A**) IC_{50} values were determined by observing binding of the inhibitor in a dilution series at various time points. (**B**) The displacement of Kinase Tracer 178 could be monitored in real time at various concentrations of inhibitor. The assay used a Eu–anti-GST antibody.

Measuring on–off binding rates

Many so-called allosteric inhibitors (which include type II inhibitors) are also characterized by a slow compound on-rate, due to the compound preferentially binding to a conformation of the kinase that is in equilibrium with other forms. Although the on-rate can be measured by monitoring the activity of the kinase at various time points after preincubating the kinase and inhibitor, it is substantially simpler to monitor binding directly, as shown in Figure 3, in which the binding of the type II inhibitor BIRB-796[2] to p38α was monitored over time using the LanthaScreen® assay.

Efficient assay of previously challenging targets

The LanthaScreen® Eu kinase binding assay platform enables researchers to assay previously challenging targets, whether for inclusion in broad selectivity studies or for primary and secondary screening. In addition, the rapid, efficient assessment of inhibitors via fluorescent assays can now be applied to kinases of multiple conformational states, active and nonactivated. To learn more about the LanthaScreen® Eu kinase binding assay and find out which products are right for your kinase, visit at **www.invitrogen.com/bp58**. ■

References

1. Liu, Y. and Gray, N.S. (2006) *Nat Chem Biol* 2:358–364.
2. Pargellis, C. et al. (2002) *Nat Struct Biol* 9:268–272.

Product	Quantity	Cat. no.
Kinase Tracer 236, 50 µM	25 µl	PV5592
Kinase Tracer 178, 25 µM	25 µl	PV5593
LanthaScreen® Eu-anti-GST Antibody	25 µg	PV5594
	1 mg	PV5595
LanthaScreen® Eu-anti-His-tag Antibody	25 µg	PV5596
	1 mg	PV5597

High-throughput chloride channel screening

INTRODUCING THE NEWEST MEMBER OF THE PREMO™ FAMILY: PREMO™ HALIDE SENSOR.

Chloride channels are involved in cellular processes as important and diverse as transepithelial transport, electrical excitability, muscle tone, and cell volume regulation.[1] In light of the physiological significance of these channels, defects in their activity can have severe implications, including such conditions as cystic fibrosis and neuronal degeneration. Moreover, a number of neuroactive drugs for mood disorders [1] target neuronal chloride channels. Despite the broad medical relevance of chloride channelopathies, researchers have struggled to find tools to screen potential therapeutic agents with the requisite precision and in sufficiently high throughput.

Modulators of chloride channels are typically screened using techniques such as whole-cell patch clamp recordings, organic dyes, or silver chloride precipitation. However, these tools lack the throughput, sensitivity, or contextual richness to be practical and robust tools for screening diverse compound libraries. High-throughput fluorescence plate reader platforms, using sensors such as FluxOR™ assays for potassium channels and Fluo-4 NW or Premo™ Cameleon Calcium Sensor for calcium channels, are particularly useful for scaling up ion channel screening efforts.[2–4] Chloride channels, however, have proven difficult to assay in such a format. Here we introduce a novel chloride sensor—Premo™ Halide Sensor—that offers researchers a tool for accurate and reliable high-throughput screening of chloride channel modulators.

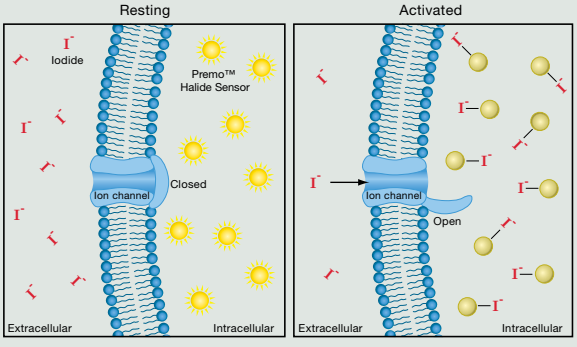

Figure 1—Principle of the Premo™ Halide Sensor: iodide redistribution upon chloride channel activation. Basal fluorescence from Premo™ Halide Sensor is high when chloride channel activity is low. Activation (opening) of chloride channels allows iodide to enter the cell, quenching the fluorescence from Premo™ Halide Sensor.

Premo™ Halide Sensor assay principle

Premo™ Halide Sensor is based on a green fluorescent protein (GFP) variant whose fluorescence, through mutations, has been rendered sensitive to halide ions.[5] Of all the spectral GFP variants, the red-shifted yellow fluorescent protein (YFP) is particularly sensitive to changes in pH and anion concentration.[6,7] Premo™ Halide Sensor uses the Venus variant of *Aequorea victoria* GFP, which displays enhanced fluorescence and increased folding with a decreased maturation time.[8] The same mutations reported by Verkman and colleagues to increase the halide sensitivity of YFP [5,7,9] have been made to the Venus sequence in the Premo™ Halide Sensor.

Chloride channels are freely permeable to iodide, and because iodide is normally not abundant in the cellular environment, very high iodide concentration gradients can be created across the cell membrane by adding it to the extracellular medium (Figure 1). By employing iodide as a surrogate ion, the Premo™ Halide Sensor maximizes the sensitivity of the fluorescent protein to chloride channel activity. The Premo™ Halide Sensor kit includes a stimulus buffer containing iodide; chloride channel opening is detected by a fluorescence decrease, or quenching (Figure 1). The surrogate ion approach is also used in the FluxOR™ Thallium Detection Kit to detect potassium channel opening.

Premo™ Halide Sensor shows an excitation and emission profile similar to YFP (Figure 2) and can therefore be detected using standard GFP/FITC or YFP filter sets. Iodide-sensitive fluorescent proteins have been successfully used in high-throughput screening (HTS) applications to screen activators of the cystic fibrosis transmembrane regulator (CFTR),[10–14] calcium-activated chloride channels,[15] and GABA A

receptor chloride channels.[16] Premo™ Halide Sensor is highly sensitive to changes in intracellular halide concentration, exhibiting a much greater quenching response to iodide than to chloride (Figure 3).

BacMam delivery for high transduction efficiency

Premo™ sensors are delivered to mammalian cells using BacMam technology,[17–18] which uses a baculovirus to deliver genes to mammalian cells. BacMam technology offers high transduction efficiency across a broad range of cell types—including primary and stem cells—as compared to other gene delivery methods. In addition, baculovirus-mediated gene delivery is safe (the insect virus is nonreplicating in mammalian cells) and does not cause observable cytopathic effects. This technology offers increased assay flexibility, allowing cotransduction of several BacMam reagents as well as modulation of expression level by varying dose and biological context. BacMam delivery uses a simple yet effective workflow, and cells can be pretransduced, then frozen, to provide assay-ready cells whenever they are required.

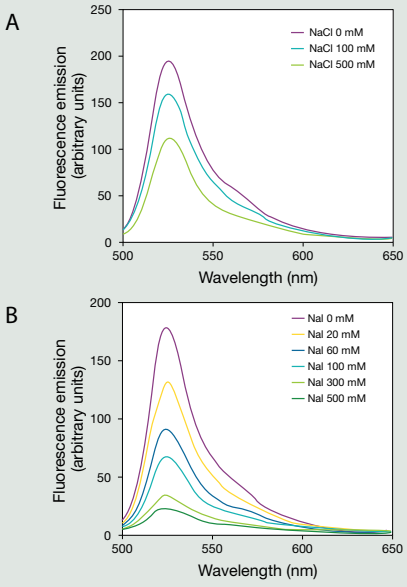

Figure 3—Quenching of Premo™ Halide Sensor fluorescence by increasing concentrations of iodide and chloride. U2OS cells were transduced with Premo™ Halide Sensor. After 24 hours, cells were trypsinized and lysed by resuspension in sterile distilled water. Fluorescence quenching of the lysate was examined using increasing concentrations of NaCl (**A**) and NaI (**B**). Iodide induces substantially greater quenching of Premo™ Halide Sensor fluorescence than chloride.

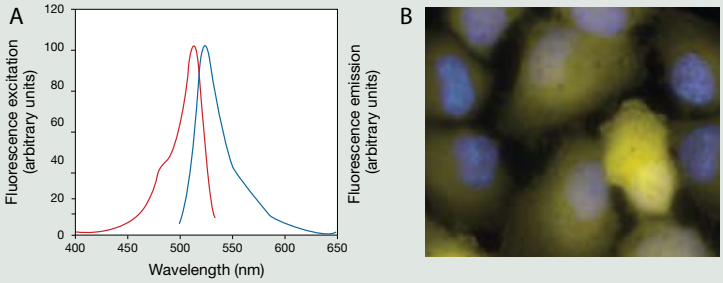

Figure 2—Expression of Premo™ Halide Sensor in U2OS cells. (**A**) Fluorescence excitation (red) and emission (blue) spectra for Premo™ Halide Sensor. (**B**) Expression of Premo™ Halide Sensor in U2OS cells counterstained with Hoechst 33342.

A true no-wash assay for HTS of chloride channels

The Premo™ Halide Sensor kit features a ready-to-use solution of virus for robust and reproducible high-throughput screening of chloride channel activity on fluorescence plate readers or fluorescence microscopes. The Premo™ Halide Sensor enables high-throughput screening of chloride channels with reproducible IC_{50} values, and real-time kinetic measurements allowing reliable, reproducible, and informative assessment of the modulation of chloride channel conductance. Moreover, the use of BacMam delivery technology means that Premo™ Halide Sensor is a true no-wash assay for chloride channels, offering sensitivity, reliability, and precision that were previously unavailable to researchers screening chloride channels. For more information about Premo™ Halide Sensor, visit **www.invitrogen.com/bp58**. ■

References

1. Jentsch, T.J. et al. (2001) *Physiol Rev* 82:503–568.
2. Terstappen, G.C. (2005) *Drug Discov Today* 2:133–140.
3. Molokanova, E. and Savchenko, A. (2008) *Drug Discov Today* 13:14–22.
4. Hanson, G.T. and Hanson, B.J. (2008) *Comb Chem High Throughput Screen* 11:505–513.
5. Galietta, L.J. et al. (2001) *FEBS Lett* 499:220–224.
6. Elsliger, M.A. et al. (1999) *Biochemistry* 38:5296–5301.
7. Wachter, R.M. and Remington, S.J. (1999) *Curr Biol* 9:R628–R629.
8. Nagai, T. et al. (2002) *Nat Biotech* 20:87–90.
9. Jayaraman, S. et al. (2000) *J Biol Chem* 275:6047–6050.
10. Ma, T. et al. (2002) *J Biol Chem* 277:37235–37241.
11. Yang, H. et al. (2003) *J Biol Chem* 278:35079–35085.
12. Galietta, L.V. et al. (2001) *Am J Physiol Cell Physiol* 281:C1734–C1742.
13. Pedemonte, N. et al. (2005) *Mol Pharmacol* 68:1736–1746.
14. Xu, L.N. et al. (2008) *Clin Exp Pharmacol Physiol* 35:878–883.
15. De La Fuente, R. et al. (2007) *Mol Pharmacol* 73:758–768.
16. Kruger, W. et al. (2005) *Neurosci Lett* 380:340–345.
17. Kost, T.A. et al. (2007) *Drug Disc Today* 12:396–403.
18. Ames, R.S. at el. (2007) *Expert Opin Drug Discov* 2:1669–1681.

Product	Quantity	Cat. no.
Premo™ Halide Sensor for 10 microplates	1 kit	P10229

Fluorescence technologies for high-content imaging and analysis

CELL HEALTH AND TOXICITY ASSAYS.

High-content imaging and analysis offers the benefits of spatially resolved and multiparametric interrogation of cells in heterogeneous populations. These advantages are particularly evident in studies related to cellular stress and death—richer data sets can provide more conclusive results and help define the next series of questions in characterizing mechanisms of toxicity. Identifying cellular events related to stress and death is critical to understanding both prelethal and lethal aspects of mechanisms associated with cytotoxicity. Understanding the off-target effects of lead compounds lends reliability and robustness to more comprehensive toxicological profiling and enables the generation of decision-making indices in the drug development process.

To effectively employ this approach, researchers need fluorescent probes that are both robust and compatible with the higher-throughput workflow of high-content imaging. These probes include components of validated high-content screening (HCS) assays as well as segmentation tools to identify nuclear and cytoplasmic regions, such as the HCS NuclearMask™ and HCS CellMask™ stains. Furthermore, when the probes used in fluorescent assays for detection of off-target drug effects are fixable and detergent resistant, they offer added value by enabling antibody detection of on-target effects in the same cell. Invitrogen continues to lead in the invention of novel fluorescent reagents for imaging and in the technical expertise to support these reagents for an extensive range of cell-based applications.

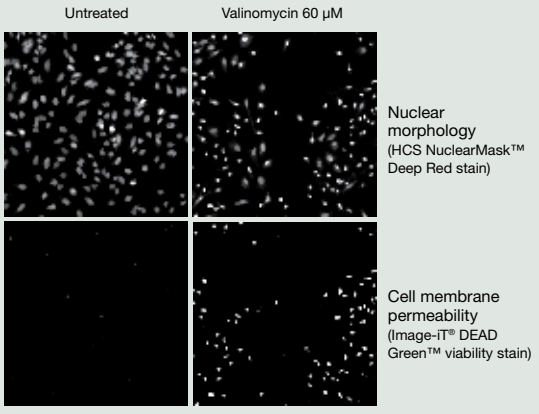

Figure 1—Cell viability assay using components of the HCS LIVE/DEAD® Green Kit. HeLa cells were left untreated or treated with 60 µM valinomycin for 24 hr, then toxicity was assayed using the Image-iT® DEAD Green™ viability stain. The HCS NuclearMask™ Deep Red stain was used for nuclear segmentation.

Viability: The fundamentals of cell health and toxicity

The HCS LIVE/DEAD® Green Kit (Cat. no. H10290) is an ideal means to measure cell viability in high-content imaging. This kit features options for total cell demarcation, including HCS NuclearMask™ Deep Red stain (Cat. no. H10294) and Image-iT® DEAD Green™ viability stain (Cat. no. I10291) for discrimination of dead cells based on plasma membrane integrity (Figure 1). Both probes bind to nucleic acids, and because signals are retained adequately after fixation and permeabilization, this assay may be combined with antibody labeling. Hoechst 33342 is also provided in the kit as a nuclear segmentation tool to maximize multiplex options.

Mitochondrial health: A sensitive indicator of cell stress

The use of reduced nicotinamide adenine dinucleotide (NADH) by Complex I of the mitochondrial respiratory chain results in oxidation of NADH, reduction of the electron carrier ubiquinone, and transport of protons from the mitochondrial matrix to the intermembrane space. This oxidoreductase activity propagates mitochondrial electron transport chain activity and generation of an electrochemical proton gradient across the inner mitochondrial membrane, which drives the phosphorylation of ADP to form ATP at Complex V. The extent to which the inner membrane is polarized is an indication of mitochondrial membrane potential and overall mitochondrial health. Depolarization

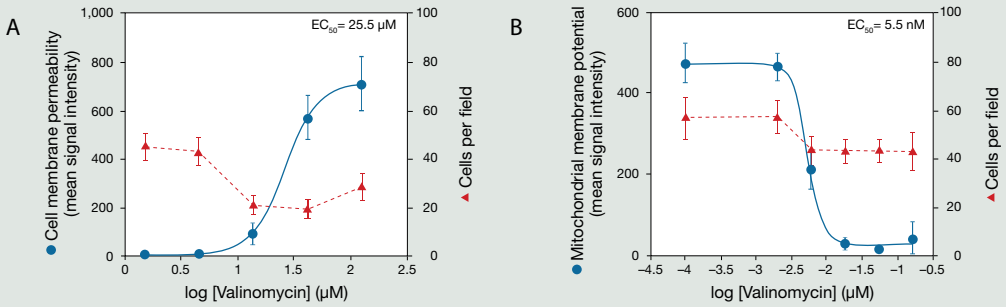

Figure 2—Dose response for valinomycin in HeLa cells determined using the HCS Mitochondrial Health Kit. HeLa cells were treated with valinomycin at final concentrations between 2 nM and 120 µM. Cells were incubated for 24 hr and assayed using the kit. Dose-response curves generated by nonlinear regression were used to determine EC_{50} values for valinomycin-induced loss of plasma membrane integrity (**A**) and mitochondrial membrane potential (**B**) with increasing concentrations of valinomycin. Cell loss with increasing drug concentrations is shown in both panels. Data points represent averages from 8 wells and error bars show standard deviations. Because valinomycin is less soluble in DMSO at concentrations above 120 µM, data points beyond this concentration are not shown.

is a good indicator of mitochondrial dysfunction, which has been increasingly implicated in drug toxicity.[1–6]

The HCS Mitochondrial Health Kit (Cat. no. H10295) was developed for simultaneous quantitative measurements of mitotoxicity and cytotoxicity in the same cell by high-content imaging and analysis (Figure 2). The MitoHealth stain included in the kit accumulates in the mitochondria of live cells in proportion to the mitochondrial membrane potential, while the Image-iT® DEAD Green™ viability stain enables discrimination of dead cells based on plasma membrane integrity. Hoechst 33342, which stains DNA in live and dead cells, is also provided in this kit as a segmentation tool to identify nuclei during automated image analysis. Cell staining is retained after formaldehyde fixation and detergent permeabilization and is amenable to subsequent immunocytochemical detection of additional targets.

DNA damage: A fork in the road for the cell stress response

A double-strand break (DSB) in chromosomal DNA is a potentially lethal lesion.[7] One of the earliest known responses to DSB formation is phosphorylation of H2A histones.[8] DNA-damaging agents induce phosphorylation of histone variant H2AX at Ser139, leading to formation of DNA foci at the site of DNA DSBs.[9] Phosphorylated H2AX aids in the recruitment of proteins responsible for DSB repair.[10] In mammalian cells, phosphatidylinositol 3 kinase–like protein kinases such as ATM (ataxia telangiectasia mutated), ATR (ATM- and Rad3-related), and DNA-PKcs (DNA-dependent protein kinase catalytic subunit) phosphorylate histone variant H2AX.[11]

The HCS DNA Damage Kit (Cat. no. H10292) was developed for simultaneous quantitative measurements of genotoxicity and cytotoxicity in the same cell by high-content imaging and analysis (Figure 3). DNA damage is measured as an indication of genotoxicity and is accomplished by specific antibody-based detection of phosphorylated H2AX (Ser139) in nuclei. A highly cross-adsorbed secondary antibody conjugated to →

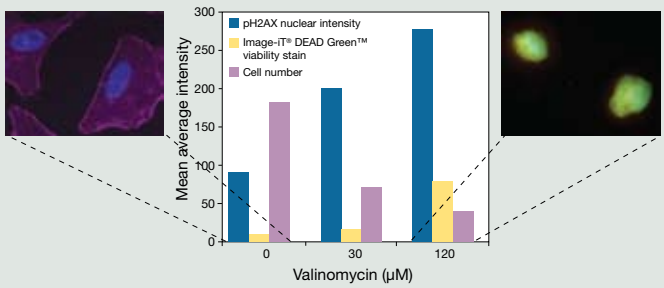

Figure 3—Detection of genotoxicity and cytotoxicity in valinomycin-treated A549 cells using the HCS DNA Damage Kit. A549 cells were treated with 30 µM or 120 µM valinomycin for 24 hr before performing the assay. With increasing concentrations of valinomycin, cells showed genotoxic effects as indicated by detection with a pH2AX antibody labeled with Alexa Fluor® 555 goat anti–mouse IgG (orange fluorescence), and cytotoxic effects as indicated by staining with the Image-iT® DEAD Green™ viability stain (green fluorescence). Blue-fluorescent Hoechst 33342 was used as a nuclear segmentation tool, and Alexa Fluor® 647 phalloidin was used to visualize F-actin (pseudocolored magenta). The image on the left shows untreated cells with intact F-actin cytoskeletons and no evidence of cytotoxicity or genotoxicity. The image on the right shows cells treated with 120 µM valinomycin, which completely disrupted the actin cytoskeletons, increased levels of DNA damage, and compromised plasma membrane integrity.

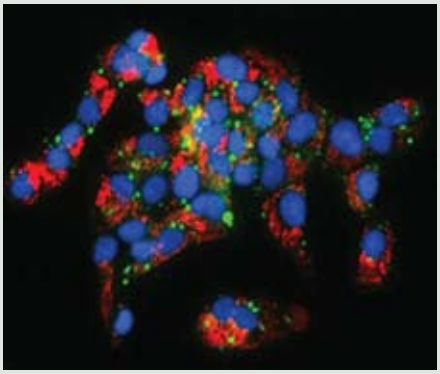

Figure 4—Multiplex detection of phospholipidosis and steatosis in HepG2 cells. Tamoxifen-treated HepG2 cells were co-incubated with HCS LipidTOX™ Red phospholipidosis detection reagent before fixation and staining with HCS LipidTOX™ Green neutral lipid stain and Hoechst 33342.

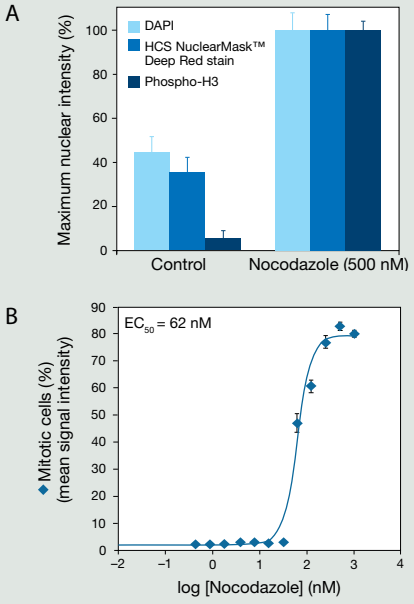

Figure 5—Imaging of nocodazole-induced mitotic arrest in A549 cells using the HCS Mitotic Index Kit. (**A**) Quantitation of cells treated with 500 nM nocodazole for 24 hr. Nuclear segmentation and DNA content were measured using DAPI or HCS NuclearMask™ Deep Red stain. The strong increase in both phospho-histone 3 and DNA staining is indicative of mitotic cells. (**B**) Dose response to 0–1,000 nM nocodazole after 24 hr incubation. The curve generated by nonlinear regression was used to determine the EC_{50} value for nocodazole.

Alexa Fluor® 555 dye is provided for sensitive immunocytochemical target detection. Image-iT® DEAD Green™ viability stain and Hoechst 33342 are also provided in the kit for detecting lethal cytotoxicity.

Phospholipidosis and steatosis: Perturbations to lipid metabolism

Phospholipidosis, the intracellular accumulation of phospholipids, is often triggered by cationic amphiphilic drugs, and can be detected when cells are incubated in the presence of phospholipids conjugated to fluorescent dyes. Steatosis, the intracellular accumulation of neutral lipids, is often triggered by drugs that affect the metabolism of fatty acids, neutral lipids, or both, and can easily be traced with HCS LipidTOX™ neutral lipid stains. Figure 4 shows simultaneous detection of phospholipidosis and steatosis using HCS LipidTOX™ reagents. These reagents are available in a range of colors and as stand-alone reagents (Cat. no. H34350, H34351, H34475, H34476, H34477) or as components of multiplex kits (Cat. no. H34157, H34158), complete with segmentation tools and compounds to use as positive controls for the induction of phospholipidosis and steatosis.

Cell cycle: Cytotoxicity and the induction of mitotic arrest or progression

Histones are core proteins of chromatin in eukaryotic cells. The histones are organized as octamers, around which the DNA is wrapped. The phosphorylation of histone 3 (H3) is involved in condensation of chromatin during mitosis and reaches a peak during mitosis. Mitotic H3 phosphorylation occurs at Ser10 of the amino terminus, and there is a tight correlation between H3 (Ser10) phosphorylation, chromosome condensation, and segregation during mitosis.[12–14] This event can serve as an indication of mitotic progression or inhibition within the context of drug profiling.

The HCS Mitotic Index Kit (Cat. no. H10293) was developed to measure mitotic cells using automated imaging and analysis and can be combined with other measurements such as DNA profiling, general cytotoxicity, or immunocytochemical detection of choice targets. The kit provides a primary antibody against H3 (pS10) as a sensitive index of mitosis, and a secondary antibody conjugated to Alexa Fluor® 488 dye. Two choices for DNA profiling and cell demarcation for image analysis, DAPI and HCS NuclearMask™ Deep Red stain (Cat. no. H10294), are also included in the kit. The HCS Mitotic Index Kit is a powerful image-based assay for the identification of compounds that affect mitotic progression (Figure 5).

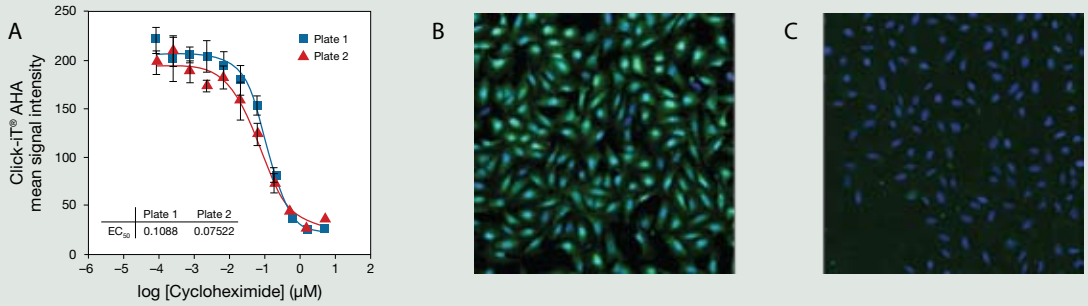

Figure 6—Detection of protein synthesis inhibition using the Click-iT® AHA Alexa Fluor® 488 Protein Synthesis HCS Assay. (**A**) Dose response curves, performed in duplicate. U2OS cells were treated in L-methionine–free medium containing 50 µM Click-iT® AHA and cycloheximide (85 pM–5 µM) for 30 min. Images show untreated cells (**B**) and cells treated with 150 µM cycloheximide (**C**).

Nascent protein synthesis and cytotoxicity

The ability to detect newly synthesized proteins or changes in protein expression resulting from disease or drug treatments is an important aspect of assessing cytotoxicity. The Click-iT® AHA Alexa Fluor® 488 Protein Synthesis HCS Assay (Cat. no. C10289) provides a fast, sensitive, nontoxic, and nonradioactive method for the detection of nascent protein synthesis [15,16] by high-content imaging and analysis (Figure 6).

Click-iT® AHA is an amino acid analog of methionine containing an azido moiety. In a manner analogous to incorporation of ^{35}S-methionine, Click-iT® AHA is added to cultured cells, where it is incorporated into proteins during active protein synthesis. Detection of the incorporated amino acid analog uses a specific covalent click chemistry reaction [17] between an azide and an alkyne, where the azido-modified protein is detected with Alexa Fluor® 488 alkyne.

A variety of cell-based assays for sound decision making

Invitrogen's expanding menu of easy-to-use fluorescence assays for automated high-content imaging and analysis offers the flexibility to interrogate very specific aspects of cytotoxicity or multiple aspects simultaneously. These powerful tools provide reliable quantitative results for decision making in the drug development process. For more information about these and many other cell health and toxicity assays, visit **www.invitrogen.com/bp58**. ■

References

1. Tirmenstein, M.A. et al. (2002) *Toxicol Sci* 69:131–138.
2. Amacher, D.E. (2005) *Curr Med Chem* 12:1829–1839.
3. O'Brien, P.J. et al. (2006) *Arch Toxicol* 80:580–604.
4. Dykens, J.A. and Will, Y. (2007) *Drug Discov Today* 12:777–785.
5. Dykens, J.A. et al. (2008) *Toxicol Sci* 103:335–345.
6. Abraham, V.C. et al. (2008) *J Biomol Screen* 13:527–537.
7. Nikiforova, M.N. et al. (2001) *Science* 290:138–141.
8. Vamvakas, S. et al. (1997) *Crit Rev Toxicol* 27:155-174.
9. Richardson, C. and Jasin, M. (2000) *Nature* 405:697–700.
10. Karran, P. (2000) *Curr Opin Genet Dev* 10:144–150.
11. Khanna, K.K. and Jackson, S.P. (2001) *Nat Genet* 27:247–254.
12. Goto, H. et al. (1999) *J Biol Chem* 274:25543–25549.
13. Johansen, K.M. and Johansen, J. (2006) *Chromosome Res* 14:393–404.
14. Hirota, T. et al. (2005) *Nature* 438:1176–1180.
15. Dieterich, D.C. et al. (2006) *Proc Natl Acad Sci U S A* 103:9482–9487.
16. Dieterich, D.C. et al. (2007) *Nat Protoc* 2:532–540.
17. Kolb, H.C. et al. (2001) *Angew Chem Int Ed Engl* 40:2004–2021.

Product	Quantity	Cat. no.
CellMask™ Deep Red Plasma Membrane Stain, 5 mg/ml solution in DMSO	100 µl	C10046
CellMask™ Orange Plasma Membrane Stain, 5 mg/ml solution in DMSO	100 µl	C10045
Click-iT® AHA Alexa Fluor® 488 Protein Synthesis HCS Assay, 2-plate size	1 each	C10289
HCS CellMask™ Deep Red Cytoplasmic/Nuclear Stain	1 set	H34560
HCS DNA Damage Kit, 2-plate size	1 each	H10292
HCS LipidTOX™ Green Phospholipidosis Detection Reagent, 1000X aqueous solution, 10-plate size	1 each	H34350
HCS LipidTOX™ Phospholipidosis and Steatosis Detection Kit, 2-plate size	1 kit	H34157
HCS LipidTOX™ Phospholipidosis and Steatosis Detection Kit, 10-plate size	1 kit	H34158
HCS LipidTOX™ Red Phospholipidosis Detection Reagent, 1000X aqueous solution,10-plate size	1 each	H34351
HCS LipidTOX™ Green Neutral Lipid Stain, solution in DMSO	1 each	H34475
HCS LipidTOX™ Red Neutral Lipid Stain, solution in DMSO	1 each	H34476
HCS LipidTOX™ Deep Red Neutral Lipid Stain, solution in DMSO	1 each	H34477
HCS LIVE/DEAD® Green Kit, 2-plate size	1 each	H10290
HCS Mitochondrial Health Kit, 2-plate size	1 each	H10295
HCS Mitotic Index Kit, 2-plate size	1 each	H10293
HCS NuclearMask™ Deep Red stain, 250X concentrate in DMSO	400 µl	H10294
Image-iT® DEAD Green™ viability stain, 1 mM solution in DMSO	25 µl	I10291

Novel solid-phase antibody labeling

TAKE ADVANTAGE OF THE SPEED, EFFICIENCY, AND CONVENIENCE OF APEX ANTIBODY LABELING KITS.

Many IgG antibodies are available only in small quantities and are packaged with stabilizing proteins, such as bovine serum albumin (BSA), or other contaminants. These contaminants can interfere with the amine-reactive labeling reagents used to covalently attach a fluorophore to an antibody, and removing these contaminants can cause significant antibody loss. The new APEX Antibody Labeling Kits provide a convenient means of directly labeling a very small amount of IgG antibody (10–20 µg) with a fluorophore, while allowing you to easily remove contaminants without losing antibody.

Lose contaminants without sacrificing antibody

The APEX Antibody Labeling Kits use a solid-phase labeling technique that captures the IgG antibody on the resin inside the APEX antibody labeling tip (Figure 1). Any contaminants, including stabilizing proteins or amine-containing buffers, are simply eluted through the tip. After applying the amine-reactive label, a fluorescent IgG conjugate is ready for use in an imaging (Figures 2 and 3) or flow cytometry application in as little as 2.5 hours with very little hands-on time.

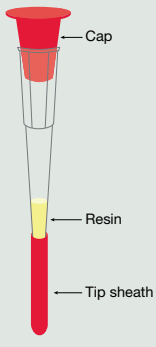

Figure 1—Diagram of an APEX antibody labeling tip.

Eliminate background fluorescence, gain flexibility

Although secondary antibodies may offer a brighter fluorescent signal, using directly labeled antibodies eliminates the background fluorescence commonly observed when secondary antibodies bind nonspecifically to the sample. In addition, directly labeled antibodies allow you to use more than one same-species antibody in a single staining experiment.

Start labeling today

The APEX antibody labeling kits include all of the reagents necessary to perform five separate labeling reactions of 10–20 µg of IgG antibody with superior Molecular Probes® fluorophores, some of which can be used as alternatives to biotin (Table 1). Unlike biotin, which is an endogenous ligand in mitochondria, dye-based haptens permit background-free staining of cells and tissues. Other available Molecular Probes® antibody and protein labeling kits are optimized for noncovalent labeling of smaller or larger amounts of IgG antibodies or proteins >30 kDa (Table 2). Learn more at **www.invitrogen.com/bp58**. ■

Table 1—Spectral characteristics and applications of the fluorescent labels available in the APEX Antibody Labeling Kits.

Label	Abs*	Em*	Application
Alexa Fluor® 488	495	518	Fluorescent label for use in imaging or flow cytometry; hapten for signal amplification with anti–Alexa Fluor® 488 antibodies
Alexa Fluor® 555	555	565	Fluorescent label for use in imaging
Alexa Fluor® 594	590	617	Fluorescent label for use in imaging
Alexa Fluor® 647	650	665	Fluorescent label for use in imaging or flow cytometry
Oregon Green® 488	496	524	Fluorescent label for use in imaging or flow cytometry; hapten for signal amplification with anti–fluorescein/Oregon Green® antibodies
Pacific Blue™	416	451	Fluorescent label for use in imaging or flow cytometry

* Absorption (Abs) or fluorescence emission (Em) maxima, in nm.

Table 2—Molecular Probes® antibody and protein labeling kits.

Amount of IgG	Product	Key features
<1–20 µg	Zenon® IgG Labeling Kits	• Labeled IgG antibodies ready to use in 10 min • Isotype-specific labeling • Fast, noncovalent attachment of label • Labeling compatible with stabilizing proteins such as BSA
10–20 µg	APEX Antibody Labeling Kits	• Labeled IgG antibodies ready to use in 2.5 hr (~15 min hands-on time) • Covalent attachment of label • Labeling compatible with stabilizing proteins such as BSA
20–100 µg	Microscale Protein Labeling Kits	• Labeled antibodies or other proteins ready to use in 2 hr (~30 min hands-on time) • Covalent attachment of label • Optimized for proteins between 10 and 150 kDa, including IgG antibodies (~150 kDa) • Stabilizing proteins must be removed from sample before labeling
100 µg	Monoclonal Antibody Labeling Kits	• Labeled IgG antibodies ready to use in 90 min (~15 min hands-on time) • Covalent attachment of label • Optimized for IgG antibodies (~150 kDa) • Stabilizing proteins must be removed from sample before labeling • Designed to label polyclonal and monoclonal IgG antibodies
1 mg	Protein Labeling Kits	• Labeled antibodies ready to use in 2 hr (~30 min hands-on time) • Covalent attachment of label • Optimized for IgG antibodies (~150 kDa) • Stabilizing proteins must be removed from sample before labeling
0.3–5 mg	SAIVI™ Antibody Labeling Kits	• Labeled IgG antibodies ready to use in 90 min (~10 min hands-on time) • Covalent attachment of label • Optimal degree of labeling for *in vivo* imaging applications • Labeled antibodies ready for use in applications that require azide-free reagents, such as live-cell imaging or direct injection into animals

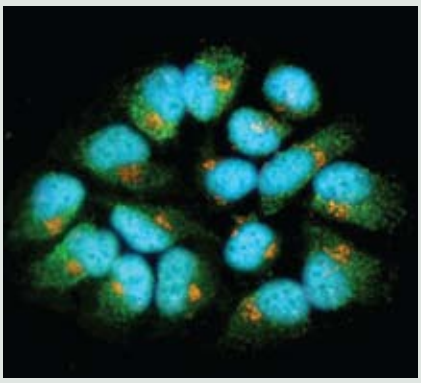

Figure 2—Mitochondrial and Golgi complex labeling in HeLa cells. Fixed and permeabilized HeLa cells were treated with multiple mouse primary antibodies directly conjugated using APEX Alexa Fluor® Antibody Labeling Kits. The Golgi apparatus was detected with an anti–golgin-97 mouse monoclonal antibody labeled using the APEX Alexa Fluor® 555 Antibody Labeling Kit (Cat. no. A10470, orange fluorescence). Mitochondria were detected with an anti–OxPhos Complex V inhibitor protein mouse IgG1 monoclonal antibody labeled using the APEX Alexa Fluor® 488 Antibody Labeling Kit (Cat. no. A10468, green fluorescence). Nuclei were stained with blue-fluorescent DAPI (Cat. no. D1306, D3571, D21490).

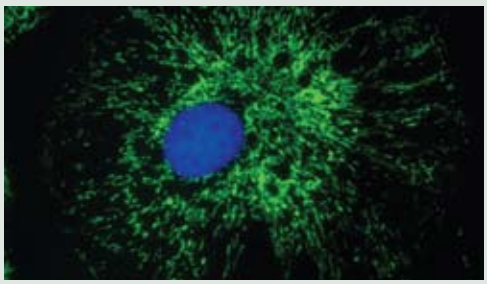

Figure 3—Mitochondrial labeling in bovine pulmonary artery endothelial (BPAE) cells. Fixed and permeabilized BPAE cells were treated with an anti–OxPhos Complex V inhibitor protein mouse IgG1 monoclonal antibody labeled using the APEX Alexa Fluor® 488 Antibody Labeling Kit (Cat. no. A10468, green fluorescence) to detect mitochondria. Nuclei were stained with blue-fluorescent DAPI (Cat. no. D1306, D3571, D21490).

Product	Quantity	Cat. no.
APEX Alexa Fluor® 488 Antibody Labeling Kit	1 kit	A10468
APEX Alexa Fluor® 555 Antibody Labeling Kit	1 kit	A10470
APEX Alexa Fluor® 594 Antibody Labeling Kit	1 kit	A10474
APEX Alexa Fluor® 647 Antibody Labeling Kit	1 kit	A10475
APEX Oregon Green® 488 Antibody Labeling Kit	1 kit	A01476
APEX Pacific Blue™ Antibody Labeling Kit	1 kit	A10478

Automated cell counting at your fingertips

THE COUNTESS™ AUTOMATED CELL COUNTER.

Make manual cell counting a thing of the past. The Countess™ Automated Cell Counter is a new instrument that provides easy and accurate cell and viability counts. You can get the data you need about your cell cultures in just 30 seconds. Beyond the obvious benefit of convenience, automated cell counting provides increased accuracy, better downstream results, time savings, and expanded experimental possibilities.

Accuracy you can count on

The Countess™ Automated Cell Counter (Figure 1) uses trypan blue staining combined with a sophisticated image analysis algorithm to count all cells in a sample—even mildly clumpy samples—as well as assess viability and measure average cell size. The Countess™ instrument produces accurate cell and viability counts and completes all calculations in 30 seconds (Figure 2) using as little as 5 µl of your sample. A cell viability percentage is calculated automatically. The measurement range extends from 1 x 10^4 to 1 x 10^7 cells/ml, with an optimal range from 1 x 10^5 to 4 x 10^6 cells/ml, broader than that of a hemocytometer (Figure 3). The instrument counts cell size from 5 to 60 µm and counts beads from 4.5 to 60 µm. We have tested more than 20 commonly used cell types including primary cells, blood cells, yeast cells (without viability assessment), insect cells, and fish cells. For a list of validated cell lines as well as frequently asked questions about cell counting capabilities, visit **www.invitrogen.com/countess**.

Counting only 100 cells gives you an accuracy of about 10%. Automated counting makes it easy to count 500 or 1,000 cells, giving you much higher accuracy and eliminating the subjective decisions about which cells to include in the count.

Figure 1—The Countess™ Automated Cell Counter.

Expanded experimental possibilities and data archiving functions

Automated cell counting allows you to perform experiments that are difficult or impossible to do using a hemocytometer, ensuring better results in your downstream experiments. Now you can set up dosage studies or any medium-sized experiment without worrying about the state of your data after you've been counting by hand for hours. In addition, the instrument includes data archiving functions as well as a handy dilution calculator to help you determine how to prepare your sample for your next experiment. You can archive data as a Countess™ file (.DBT) and as a .CSV file, allowing analysis with Microsoft® Excel® or another spreadsheet program. Countess™ PC software is included with the Countess™ instrument for further analysis (compatible with Windows® operating systems (Microsoft) only); with this software you can print a report for your lab notebook, so that you'll have a record of your cells on a given day.

Convenient, portable, and maintenance free

The small footprint of the Countess™ Automated Cell Counter means that your benchtop stays clutter free. Small and portable, the Countess™ instrument can simply be stowed on a shelf until you're ready to count. There's no need for dedicated bench space, and the

Countess™ instrument does not require a computer. The instrument uses disposable chamber slides, so there's no setup, cleaning, or maintenance required. The Countess™ instrument has no moving parts to maintain, no tubes to clean, and no buffers to replace. In fact, the instrument doesn't require any maintenance until the battery needs replacement in ~5 years. No downtime, no waiting for service technicians, no service contract costs—just reliable counting, sample after sample and year after year.

Figure 2—The Countess™ Automated Cell Counter workflow. (**A**) Pipette the sample into the counting slide; (**B**) insert the slide into the Countess™ instrument; (**C**) press "Count cells"; (**D**) results are displayed in 30 seconds.

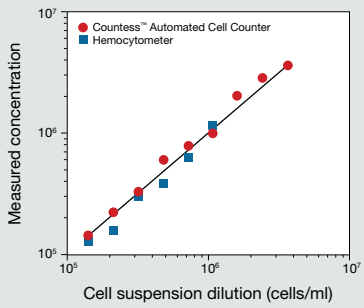

Figure 3—Countess™ instrument data extend farther along the high cell concentration range than hemocytometer readings.

Eliminate pain and fatigue

Automated counting with the Countess™ instrument reduces the eye strain, backaches, and hand cramps that manual counting can cause, and eliminates the fatigue brought on by prolonged tedious manual counting that can lead to erroneous results. Both you and your experiments will benefit.

Experience the benefits of automated counting

With the Countess™ Automated Cell Counter, you'll avoid the tedium of manual counting while enjoying the time savings, increased accuracy, and other benefits that automated counting provides. Learn more about the Countess™ instrument at **www.invitrogen.com/bp58**. ■

Product	Quantity	Cat. no.
Countess™ Automated Cell Counter*	1 each	C10227
Countess™ Cell Counting Chamber Slides†	50 slides (100 counts)	C10228
Trypan Blue Stain (0.4%)	2 ml	T10282

* Includes 50 cell counting chamber slides and trypan blue.
† For the Countess™ Automated Cell Counter; includes trypan blue.

Dynamic signaling by integrins

PROTEIN PHOSPHORYLATION AND ACTIVATION OF NETWORKS.

Integrins are single membrane–spanning glycoprotein receptors consisting of a large extracellular domain, which binds to extracellular matrix (ECM) components, and a small cytoplasmic domain, which takes part in a complex network of intracellular signaling events[1] (Figure 1). Composed of α and β subunits, integrins form structural and functional linkages between the ECM and the cytoskeleton, linker proteins, and associated signaling proteins, which include a large number of protein kinases, phosphatases, phospholipases, and small GTPases. Individual integrins facilitate binding to specific ECM proteins including fibronectin, laminins, collagens, tenascin, vitronectin, and thrombospondin. Signaling mediated by integrin–ECM interactions is integrated with the action of many other transmembrane signaling proteins to activate a wide range of cellular responses such as embryonic development, morphogenesis, angiogenesis, cytoskeletal reorganization, cellular proliferation, migration, and survival.[2–5] Here we describe some of the Invitrogen™ tools available for integrin signaling pathway research.

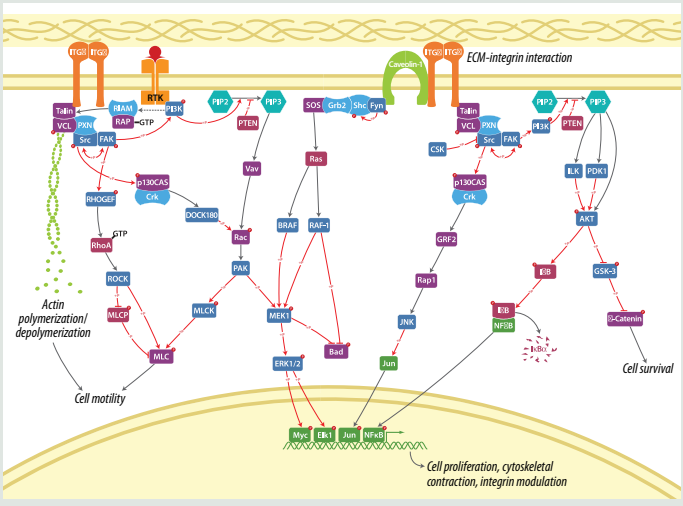

Figure 1—The integrin signaling pathway.

Inside-out signaling and phosphorylation of integrin β3

Clustering of integrin–ECM interactions forms focal adhesions, which concentrate cytoskeletal components and the signaling molecules within these clusters. Activation of these signaling complexes leads to

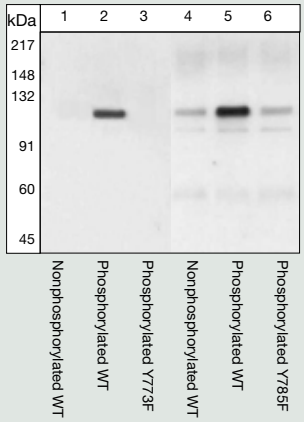

Figure 2—Western blot detection of integrin β3 phosphoregulation. From K562 cells transfected with human integrin β3, wild-type (WT, lanes 1, 2, 4, 5) or mutant (Y773F, lane 3; Y785F, lane 6) integrin β3 left untreated (lanes 1, 4) or treated with 2 mM $MnCl_2$ and 100 µM Na_3VO_4 for 10 min at 37°C to induce phosphorylation (lanes 2, 3, 5, 6) was immunoprecipitated using a 1A2 (integrin β3) monoclonal antibody (generously provided by Scott Blystone, SUNY Upstate Medical University), resolved by SDS-PAGE, and transferred to a PVDF membrane. The membrane was blocked, then incubated with integrin β3 [pY773] (lanes 1–3) or [pY785] antibody (lanes 4–6) for 2 hr at room temperature. Signals were detected using the Tropix® Western-*Star*™ system (Cat. no. T1048) after incubating the membrane with goat $F(ab')_2$ anti–rabbit IgG alkaline phosphatase (Cat. no. ALI4405). Phosphorylation was detected for wild-type but not mutant integrin β3, demonstrating the specificity of the integrin β3 [pY773] and [pY785] antibodies.

phosphorylation of critical residues within the cytoplasmic domains of integrins, triggering conversion of integrin from a low-affinity to a high-affinity activated state with respect to ECM binding—a process known as inside-out signaling.[6] For example, integrin β3 (CD61), a 130 kDa transmembrane glycoprotein that associates noncovalently with integrin α subunits (α_{IIb}, α_v) to form the functional receptor, binds with low affinity to specific extracellular matrix proteins (e.g., fibronectin, vitronectin). Phosphorylation of the human β3 integrin cytoplasmic tail at Tyr773 activates the receptor and promotes cell adhesion, while phosphorylation of Tyr785 is essential for Shc and Grb2 binding and promotes cell migration.[7] Phosphorylation of the β3 integrin cytoplasmic tail at Tyr773 and Tyr785 can be detected selectively using high-avidity phosphorylation site–specific antibodies (Figure 2).

Recruitment and activation of intracellular signaling complexes

Increased affinity for ECM components promotes the ability of integrins to recruit intracellular signaling complexes and thereby facilitate their activation. The cytoplasmic tail of integrins serves as a binding site for α-actinin and talin, which then recruit vinculin, a protein involved in anchoring F-actin to the membrane.[8] Actin dynamics can be studied in real time using Cellular Lights™ reagents (Figure 3). In addition to actin polymerization/depolymerization, ligand binding to integrins results in talin-mediated oligomerization of focal adhesion kinase (FAK), a critical regulator of focal adhesion signaling. The autophosphorylation of FAK at Tyr397, which results in activation of its intrinsic tyrosine kinase activity, can be detected using a highly selective antibody to this phosphorylation site (Figures 4 and 5). Phosphorylation at this site →

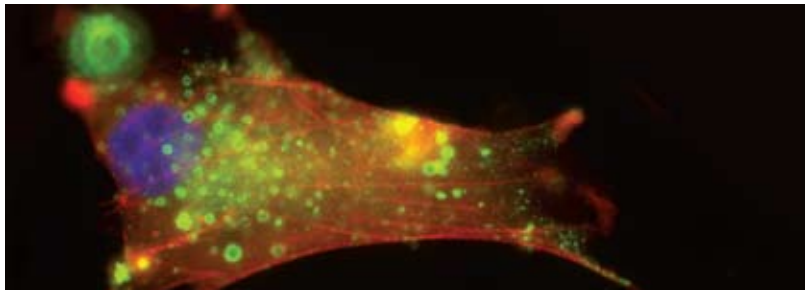

Figure 3—Actin dynamics. Cascade Biologics® human aortic smooth muscle cells (HASMC) were transduced with Cellular Lights™ Actin-RFP (red) and Organelle Lights™ Endosomes-GFP (green); nuclei were stained with blue-fluorescent Hoechst 33342.

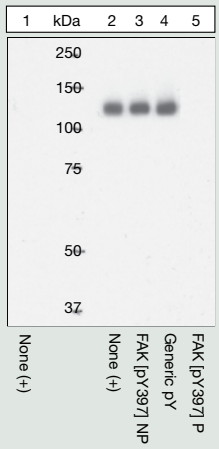

Figure 4—Validation of FAK [pY397] phosphospecific antibody. Extracts of vanadate-treated (50 µM, 16 hr) primary chicken embryo fibroblasts plated on fibronectin and expressing either FAK Y397F mutant protein (lane 1) or wild-type FAK protein (lanes 2–5) were resolved by SDS-PAGE and transferred to a PVDF membrane. The membrane was blocked, and prior to incubation with FAK [pY397] monoclonal antibody, was incubated with no peptide (lanes 1 and 2), the nonphosphorylated peptide corresponding to the phosphopeptide immunogen (lane 3), a generic phosphotyrosine-containing peptide (lane 4), or the phosphopeptide immunogen (lane 5).

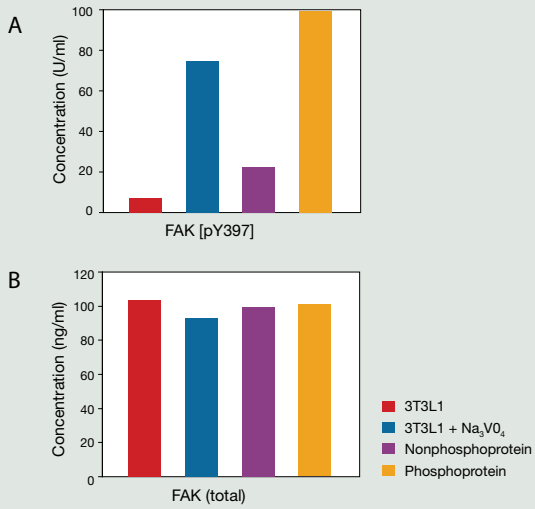

Figure 5—Detection of total and phosphorylated FAK [pY397] by ELISA. 3T3L1 cells, untreated and treated with 1 mM Na_3VO_4, were lysed and assayed in parallel for total FAK and FAK [pY397] expression. The FAK [pY397] ELISA Kit detected a phosphorylated recombinant FAK in addition to the phosphorylated FAK from treated cells, but not the corresponding nonphosphorylated forms of recombinant FAK and FAK from untreated cells (**A**). In contrast, the FAK (Total) ELISA Kit detected both phosphorylated and nonphosphorylated recombinant FAK and FAK in both treated cells and untreated controls (**B**).

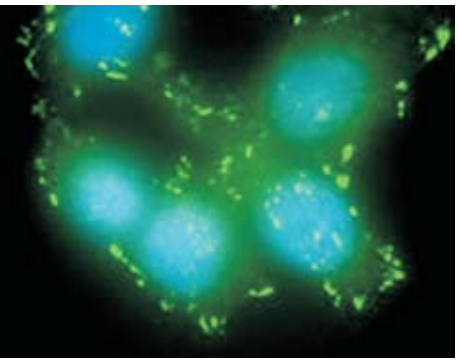

Figure 6—Detection of phosphorylated FAK [pY397] in HeLa cells. Fixed cells were immunostained with a rabbit monoclonal antibody to FAK [pY397] and visualized using a FITC-conjugated anti-rabbit secondary antibody. Nuclei were stained with blue-fluorescent DAPI. The image shows phosphorylated FAK localized at focal adhesions.

causes FAK to be localized to focal adhesion structures (Figure 6), and also serves as an important biomarker for invasion.[9] These events lead to phosphorylation at additional regulatory sites on FAK and the ability to bind and activate the Src-family kinases Src and Fyn, which in turn phosphorylate FAK and the FAK-associated proteins paxillin, tensin, and p130Cas. Activated FAK phosphorylates PI3K, PLCγ, and GRB7, leading to their activation.[10] Activation of PI3K links integrin activation with the Akt signaling pathway for activation of cell survival mechanisms.

Src phosphorylation of FAK at Tyr925 leads to the formation of a complex with GRB2 and SOS and then activation of Ras, which allows activation of numerous kinases including MEKKs, PAKs, MEKs, JNK, and SAPK. These kinases are key regulators of gene expression via the phosphorylation of multiple transcription factors including c-Myc, Elk1, Jun, and serum response factor (SRF). Activated Src also phosphorylates p130Cas, promoting the formation of a protein complex with Crk and Dock180. This protein complex increases the membrane affinity for Rac, leading to further activation of the kinase pathways mentioned above.[11] Another signaling pathway utilized by integrin for MAPK activation is via integrin association with caveolins. Caveolins are small membrane proteins (22 kDa) that can associate to form high molecular mass proteins. Caveolins contain a hydrophobic central region, which allows their embedding into the plasma membrane, with cytoplasmic N- and C-terminal domains. Caveolin-1 (Cav-1) associates with integrins and Fyn (Src-related kinase), where Cav-1 mediates the phosphorylation of Shc by Fyn. Phosphorylated Shc serves as a binding site for Grb2 and SOS and further activation of Ras and the MAPK pathway.[12]

The importance of further study

This complex network of integrin–matrix adhesion working in concert with activation of other transmembrane proteins and the corresponding downstream signaling pathways plays a fundamental role in almost all homeostasis at the level of cells, tissues, organs, and the intact body, making this an intense area of investigation for systems biology. Recognition that deregulation of integrin signaling is an important driver of human disease, especially cancer, has led to anti-adhesive strategies being actively pursued as promising therapeutic treatments.[13]

Invitrogen offers a variety of tools to facilitate research on integrin signaling and the ECM. To learn more about the integrin signaling pathway and to find assays, proteins, and other phosphospecific antibodies useful in these studies, visit **www.invitrogen.com/bp58**. ■

References

1. Wegener, K.L. and Campbell, I.D. (2008) *Mol Membr Biol* 25:376–387.
2. Serini, G. et al. (2008) *Curr Opin Hematol* 15:235–242.
3. Müller, E.J. et al. (2008) *J Invest Dermatol* 128:501–516.
4. Constantin, G. (2008) *J Neuroimmunol* 198:20–26.
5. Arcangeli, A. and Becchetti, A. (2006) *Trends Cell Biol* 16:631–639.
6. Arnaout, M.A. et al. (2007) *Curr Opin Cell Biol* 19:495–507.
7. Blystone, S.D. (2002) *J Biol Chem* 277:46886–46890.
8. Martin, K.H. et al. (2002) *Science* 296: 1652–1653.
9. Ilić, D. et al. (2001) *Am J Pathol* 159:93–108.
10. Parsons, J.T. et al. (2000) *Oncogene* 19:5606–5613.
11. Kumar, C.C. (1998) *Oncogene* 17:1365–1373.
12. Salanueva, I.J. et al. (2007) *J Cell Mol Med* 5:969–980.
13. Schmidmaier, R. and Baumann, P. (2008) *Curr Med Chem* 15:978–990.

Product	Quantity	Cat. no.
INTEGRIN β3 [pY773] PAb hu (BioSource™)	10 blots	44876G
INTEGRIN β3 [pY785] PAb hu (BioSource™)	10 blots	44878
FAK [pY397] PAb	10 blots	44624G
FAK [pY397] MAB	10 blots	44625G
FAK [pY397] ELISA Kit	96 tests	KHO0441
Cellular Lights™ Actin-RFP	1 kit	C10127
Organelle Lights™ Endosomes-GFP	1 kit	O10104
Hoechst 33342, trihydrochloride, trihydrate	100 mg	H1399

Targeting cardiovascular disease and Alzheimer's disease

BEYOND REGULATING CHOLESTEROL LEVELS, NEW DRUG TARGETS EMERGE FROM LIPID RESEARCH.

The nexus of heart and brain disease

Once considered very separate medical maladies, diseases of the brain and of the circulatory systems are now leading researchers to converge on a common set of drug targets. Extensive evidence is accumulating that these two broad categories of diseases share many common risk factors. In autopsy studies of Alzheimer's disease (AD) patients, for example, counting microvascular lesions was as predictive of the extent of the disease as counting amyloid plaques;[1] and the prevalence of AD pathology was 11 times higher in women who had died of stroke.[2]

A significant risk factor for cardiovascular disease (CVD) and AD is metabolic syndrome, characterized by a cluster of attributes including elevated waist circumference, blood pressure, triglycerides, and fasting glucose, along with reduced levels of high-density lipoproteins (HDL). Diabetes alone increases the risk for AD by 30 to 65%, and patients with metabolic syndrome have a nearly 4-fold greater probability of developing AD.[3,4] The pathophysiological basis of metabolic syndrome is complex, but it is apparent that disruption of critical regulators of lipid metabolism has dire consequences, not just for CVD[5,6] but for AD,[7] Huntington's disease, multiple sclerosis, diabetes, and more.

To investigate these critical lipid trafficking pathways, Invitrogen provides an array of Molecular Probes® reagents and assays that can be used to attack the questions from multiple entry points, from the lipid transporters themselves to the enzymes that regulate their function and levels in circulation (Table 1).

Cholesterol: Here, there, and everywhere

It is well established that blood plasma levels of cholesterol and their carrier particles—low-density lipoproteins (LDL) and HDL—play a critical role in CVD. Treatment of atherosclerosis in particular has focused on strategies for lowering overall cholesterol levels using HMG-CoA reductase inhibitory therapies or statins. Disruptions in cholesterol regulation, however, can also have consequences for the functioning of the human brain, which contains 25% of the body's cholesterol. The association of lipids with neural degeneration was first indicated by studies showing that apolipoprotein E (ApoE)-containing HDL particles were dramatically upregulated following nerve injury.[8] Later, identification of the ApoE4 allele as the first qualified risk factor for AD began the search for understanding how lipoproteins and cholesterol retention influence the consequences of amyloid burden on brain function.[9–12]

Researchers are now shifting attention from the cholesterol-lowering statin drugs to the regulation of phospholipases that line endothelial vessels, float in plasma, and complex with lipoproteins. Of the four distinct phospholipase families, phospholipase A1 (PLA1) and phospholipase A2 (PLA2)—which cleave at the SN1 site and SN2 site, respectively, in the phospholipid head group—are drawing the most interest because members of these two families modulate both the levels and toxicities of plasma HDL and LDL particles (see sidebar). These proatherogenic phospholipases are thus prime targets for controlling and monitoring the progression of many disease states. →

The tale of two phospholipases

Endothelial lipase (EL) is a cell-surface PLA1 enzyme that lines arterial blood vessel walls. Upregulated by cytokines and proinflammatory drugs, EL lowers HDL levels while elevating free fatty acids and reactive cholesterol in plasma. In extreme cases, endothelial lipase completely metabolizes HDL particles, activating peroxisome proliferator–activated receptor[1,2] (PPARalpha) and releasing the HDL-mediated repression of leukocyte adhesion.[3] Anti-inflammatory drugs can downregulate EL and reverse its effects by elevating intact healthy plasma HDL.

Lipoprotein lipase (LpL), a secreted PLA2 enzyme, is the primary enzyme acting on circulating triglycerides and oxidized LDL to form the proinflammatory lysophosphatidylcholine and oxidized nonesterified fatty acids that can lead to patchy foci of plaques on endothelial walls, which are the hallmark of nascent disease. The overexpression of this secreted PLA2 has been found to be an accurate predictor of CVD, with many researchers suggesting that PLA2 will soon replace C-reactive protein as the go-to patient diagnostic test.

References

1. White, L. et al. (2002) *Ann N Y Acad Sci* 977:9–23.
2. Tamamizu-Kato, S. et al. (2008) *Biochemistry* 47:5225–5234.
3. Ahmed, W. et al. (2006) *Circ Res* 98:490–498.

Selective phospholipase A1 and phospholipase A2 substrates

Invitrogen has introduced highly selective fluorogenic substrates for the PLA1 and PLA2 families of phospholipases. A recent paper has established the robustness and scalability of earlier less-specific versions of these compounds for ultrahigh-throughput screening of lipase inhibitors.[14] In our own studies, the new PED-A1 and Red/Green BODIPY® PC-A2 substrates show dramatically improved signal-to-noise ratios and significantly increased enzyme selectivity. Cleavage of these PLA1 and PLA2 substrates by their corresponding phospholipases produces a 20-fold increase in fluorescence (Figure 1). In addition, phospholipase assays with these new substrates can be run in real time for true kinetic analysis of enzyme rates (Figure 2).

Available separately or as part of an EnzChek® Phospholipase Assay Kit (Table 1), the PED-A1 and Red/Green BODIPY® PC-A2 substrates provide true feed-and-read assays: simply add the substrates in liposomes to the microplate wells, wait 30 minutes, and read the increase in fluorescence (or decrease, for candidate inhibitor compounds). These assays are ideal for large screens, but sensitive and selective enough for downstream lead characterization. Although these substrates are designed for microplate-based assays, studies have indicated their potential utility in whole-cell or even whole-animal studies.

Table 1—A selection of Invitrogen™ products for studying lipid disregulation in CVD and AD.

	Quantity	Cat. no.	Notes
Fluorogenic phospholipase substrates			
PED-A1	100 µg	A10070	PLA1 activity releases intramolecular quenching of the BODIPY® FL dye by DNP, yielding an increase in emission at 530 nm.
Red/Green BODIPY® PC-A2	100 µg	A10072	PLA2 activity releases a BODIPY® FL dye, resulting in decreased quenching by FRET of a BODIPY® 558/568 dye and an increase in emission detected in the range 515–545 nm.
bis-BODIPY® FL C_{11}-PC	100 µg	B7701	PLA1 or PLA2 activity releases intramolecular quenching of the two BODIPY® FL dyes, yielding an increase in emission at 512 nm.
PED6	1 mg	D23739	PLA2 activity releases intramolecular quenching of the BODIPY® FL dye by DNP, yielding an increase in emission at 511 nm.
Cholesterol assay and enzyme assays			
Amplex® Red Cholesterol Assay Kit	1 kit, 500 assays	A12216	Cholesterol is readily quantitated using this enzyme-coupled assay and a fluorescence microplate reader or fluorometer, with a detection limit of ~80 ng/ml.
Amplex® Red Monoamine Oxidase Assay Kit	1 kit, 500 assays	A12214	This enzyme-coupled assay detects as low as 12 µU/ml purified monoamine oxidase activity *in vitro* using a fluorescence microplate reader or fluorometer.
Amplex® Red Sphingomyelinase Assay Kit	1 kit, 500 assays	A12220	This enzyme-coupled assay detects ≥80 µU/ml sphingomyelinase activity *in vitro* using a fluorescence microplate reader or fluorometer.
EnzChek® Paraoxonase Assay Kit	1 kit, 100 assays	E33702	This assay detects ≥50 mU/ml paraoxonase activity *in vitro* using a fluorescence microplate reader or fluorometer.
EnzChek® Phospholipase A1 Assay Kit	1 kit, 2-plate size 1 kit, 10-plate size	E10219 E10221	This assay employs the PED-A1substrate to detect ≥0.04 U/ml PLA1 activity *in vitro* using a fluorescence microplate reader or fluorometer.
EnzChek® Phospholipase A2 Assay Kit	1 kit, 2-plate size 1 kit, 10-plate size	E10217 E10218	This assay employs the Red/Green BODIPY® PC-A2 substrate to detect ≥0.05 U/ml PLA2 activity *in vitro* using a fluorescence microplate reader or fluorometer.
EnzChek® Myeloperoxidase (MPO) Activity Assay Kit	1 kit, 400 assays	E33856	This kit provides assays for the determination of both chlorination and peroxidation activities of MPO in solution and in cell lysates.
Zen™ Myeloperoxidase (MPO) ELISA Kit	1 kit, 200 assays	Z33857	This assay detects MPO over a broad dynamic range (0.2 to 100 ng/ml) *in vitro* using a fluorescence microplate reader or fluorometer.
Unlabeled and fluorescent low-density lipoprotein (LDL) and acetylated LDL (AcLDL) particles			
Unlabeled LDL from human plasma	200 µl, 2.5 mg/ml	L3486	Fluorescent LDL is labeled with DiI or BODIPY® FL dye, highly fluorescent lipophilic dyes that diffuse into the hydrophobic portion of the LDL complex without affecting the LDL-specific binding of the apoprotein. Fluorescent LDL has been used to quantitate LDL receptors, analyze their motion and clustering, and follow their internalization.
DiI LDL	200 µl, 1 mg/ml	L3482	
BODIPY® FL LDL	200 µl, 1 mg/ml	L3483	
Unlabeled AcLDL from human plasma	200 µl, 2.5 mg/ml	L35354	AcLDL no longer binds to the LDL receptor, but instead is taken up by macrophage and endothelial cells that possess scavenger receptors specific for the modified LDL. Once the AcLDL complexes accumulate within these cells, they assume an appearance similar to that of foam cells found in atherosclerotic plaques. For some applications, the BODIPY® FL and Alexa Fluor® conjugates of AcLDL may be the preferred probes because these fluorophores are covalently bound to the modified apoprotein portion of the LDL complex and, unlike the DiI label, are not extracted during subsequent cell manipulation.
DiI AcLDL	200 µl, 1 mg/ml	L3484	
BODIPY® FL AcLDL	200 µl, 1 mg/ml	L3485	
Alexa Fluor® 488 AcLDL	200 µl, 1 mg/ml	L23380	
Alexa Fluor® 594 AcLDL	200 µl, 1 mg/ml	L35353	
Recombinant human apolipoprotein E (ApoE)			
ApoE2, rHuman	50 µg	P2002	Recombinant human isoforms of apoE are produced by baculovirus-mediated expression in the *Spodoptera frugiperda* (Sf) insect cell line, purified by affinity chromatography, and supplied in solution.
ApoE3, rHuman	50 µg	P2003	
ApoE4, rHuman	50 µg	PV2004	

Other enzymes that regulate lipid metabolism

Phospholipases are not the only players in regulating the toxicity of lipoprotein particles. Paraoxonase, made in the liver as part of lipoprotein particles, protects against the detrimental effects of oxidative damage from any source. The EnzChek® Paraoxonase Assay Kit provides a homogeneous fluorometric assay for paraoxonase's organophosphatase activity and is >10 times more sensitive than colorimetric assays.

Historically linked to immune system function, myeloperoxidase (MPO)—which produces pathogen-killing hypochlorous from chloride anion and hydrogen peroxide—has recently been identified as a key marker in coronary artery disease, where it can act as a source of reactive oxygen species contributing to increased pools of oxidized or carbamylated LDL.[15,16] The EnzChek® MPO Activity Assay Kit provides continuous assays for the determination of MPO's chlorination and peroxidation activities in solution and in cell lysates; the Zen™ MPO ELISA Kit provides accurate and sensitive quantitation of MPO's peroxidation activity in a variety of biological samples, including human serum.

In addition to these kits, Table 1 lists microplate-based assays for cholesterol, monoamine oxidase, and sphingomyelinase. The Amplex® Red Cholesterol Assay Kit was recently employed in a study of the effect of cholesterol levels on Aβ peptide production.[13] Sensitive ELISA kits for Aβ peptides as well as primary antibodies to peroxisome proliferator–activated receptor and many other key proteins can be found at our website at **www.invitrogen.com**.

Looking forward

The emergence of drug candidates that regulate not only lipid levels but also lipid toxicity may have broader implications than merely treating vascular disease.[5,6] It is conceivable that there may someday exist a single treatment regime for brain and heart diseases; statins have already been suggested as such a treatment.[7] Equally promising is the prospect that brain disease may be amenable to drugs that, while unable to cross the blood–brain barrier, can nonetheless treat the extensive vascular system in the brain. ■

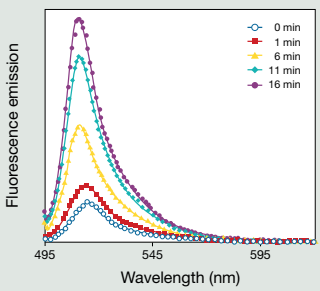

Figure 2—Real-time measurements of PLA1 activity. Fluorescence emission spectra of PED-A1 incorporated in liposomes are shown at time points after the addition of PLA1 at room temperature.

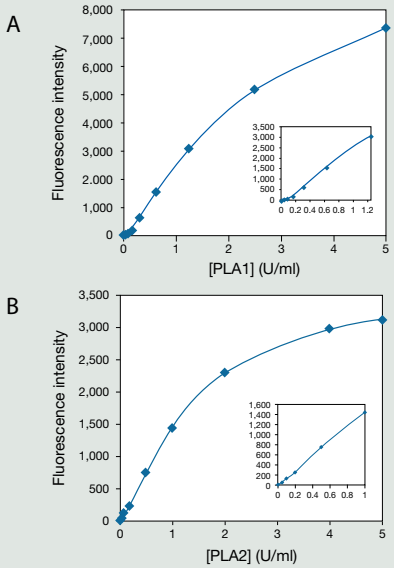

Figure 1—Fluorescence emission intensities of PLA substrates versus PLA concentration. (**A**) Plot of fluorescence emission of PED-A1 incorporated into liposomes vs. PLA1 concentration at 30 min at room temperature. (**B**) Plot of fluorescence emission of Red/Green BODIPY® PC-A2 incorporated into liposomes vs. PLA2 concentration at 10 min at room temperature. In both cases, fluorescence was measured using 460 nm excitation and 515 nm emission on a SpectraMax® M5 reader (MDS Analytical Technologies). Background fluorescence determined for the no-enzyme control reaction has been subtracted for each value.

References

1. White, L. et al. (2002) *Ann N Y Acad Sci* 977:9–23.
2. Snowdon, D.A. et al. (1997) *JAMA* 277:813–817.
3. Burdo, J.R., et al. (2008) *Neurobiol Aging* Epub ahead of print.
4. Razay, G. et al. (2007) *Arch Neurol* 64:93–96.
5. Radar, D.J. and Daugherty, A. (2008) *Nature* 451:904–913.
6. deGoma, E.M. et al. (2008) *J Am Coll Cardiol* 51:2199–2211.
7. Sagin, F.G. and Sozmen, E.Y. (2008) *Curr Alzheimer Res* 5:4–14.
8. Ignatius, M.J. et al. (1986) *Proc Natl Acad Sci U S A* 83:1125–1129.
9. Roses, A.D. (2006) *J Alzheimers Dis* 9:361–366.
10. Tamamizu-Kato, S. et al. (2008) *Biochemistry* 47:5225–5234.
11. Xiong, H. et al. (2008) *Neurobiol Dis* 29:422–437.
12. Jiang, Q. et al. (2008) *Neuron* 58:681–693.
13. Grimm, M.O. (2008) *J Biol Chem* 283:11302–11311.
14. Mitnaul, L.J. (2007) *J Lipid Res* 48:472–482.
15. Zhang, R. et al. (2001) *JAMA* 286:2136–2142.
16. Asci, G. et al. (2008) *Nephrology* (Carlton) 13:480–486.

Modeling mammary cell function in three dimensions

3D CULTURE AND BACMAM-MEDIATED TRANSDUCTION OF PRIMARY MAMMARY CELLS.

When grown in culture, normal human primary cells closely mimic the *in vivo* state of the tissue from which they were derived, providing a model cell system for dissecting complex biological processes and pathways. Invitrogen's newest primary cell offering—human mammary epithelial cells (HMEC)—opens a portal through which to observe and manipulate mammary cell function. Isolated from normal reduction mammoplasty tissue and cryopreserved at the end of the sixth culture, primary HMEC are ideal for basic and applied research, drug discovery, and the development of model systems. Each lot of primary HMEC is performance tested for viability and growth during the first culture after thaw and is guaranteed to have a lifespan of at least 16 population doublings. Here we describe 3D culture of primary HMEC using Geltrex™ Reduced Growth Factor Basement Membrane Matrix, as well as the use of BacMam technology for highly efficient transient transduction of primary HMEC with genetically encoded autofluorescent proteins.

Culture HMEC in 3D using Geltrex™ matrix

Compared with monolayer cells in 2D culture, 3D cell culture provides a much more physiologically relevant environment in which to probe cell function. Recent reports have demonstrated the value of 3D culture for modeling malignant and nonmalignant behavior of breast cancer cell lines.[1,2] Basement membranes serve as key components in 3D culture assays. These thin continuous sheets of specialized extracellular matrix separate epithelial and endothelial cells from underlying stroma and play important roles in cellular homeostasis and tissue architecture. The new Geltrex™ Reduced Growth Factor Basement Membrane Matrix is a soluble form of basement membrane (purified from Engelbreth-Holm-Swarm tumors) that can be used for 3D culture of a diverse set of cells types, including primary HMEC.

Typically, primary HMEC are first grown as standard 2D cultures, where they can be subjected to different experimental regimes. Cells are then trypsinized, seeded into 3D cultures on vessels precoated with Geltrex™ matrix, and incubated in Geltrex™ matrix diluted with complete growth medium until the desired level of acinar (spherical) structures is observed (Figure 1), usually 2–4 days under suitable conditions. A validated protocol for 3D culture of primary HMEC can be found at **www.invitrogen.com/mammarycells**. In addition, a variety of downstream applications for 3D mammary cell culture have been described, including phase-contrast and fluorescence microscopy, immunofluorescence assays, and analyses of protein and nucleic acid content.[3]

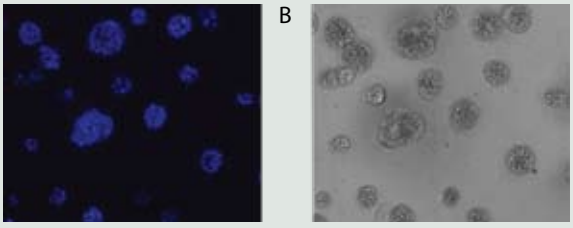

Figure 1—Fixed-cell images of primary human mammary epithelial cells grown in 3D culture using Geltrex™ Reduced Growth Factor Basement Membrane Matrix. 3D culture cells stained with the blue-fluorescent Hoechst 33342 nuclear counterstain are shown in this fluorescent micrograph (100x magnification) (**A**), and the same field of cells is shown in this phase-contrast image (**B**).

Transduce HMEC using BacMam delivery technology

A significant limitation to the wider adoption of primary cells in both academic and pharmaceutical research has been the lack of efficient, nontoxic delivery methods for transient gene expression. The BacMam delivery system is an innovative method for using recombinant baculovirus particles to introduce genes into mammalian cells, eliminating the need for lipids or dye-loading protocols that can perturb cell viability. Robust BacMam-mediated transduction provides highly reproducible and titratable expression of the gene of interest, as well as the potential for simultaneous delivery of multiple genes into a variety of

mammalian cell types. Normal human cells derived from skin (keratinocytes, melanocytes, and fibroblasts), cardiovascular tissue (aortic smooth muscle cells), and skeletal muscle have all been transduced using BacMam-mediated gene delivery, with >80% of cells expressing the encoded protein.

Organelle Lights™ and Cellular Lights™ reagents provide genetically encoded autofluorescent fusion proteins under the control of a strong constitutive promoter and prepackaged into baculovirus particles. These reagents combine the selectivity of a targeted fluorescent protein with the transduction efficiency of BacMam technology. Using Organelle Lights™ Golgi-RFP and Cellular Lights™ Actin-RFP reagents, we have successfully achieved highly efficient, discrete, and transient labeling of the Golgi apparatus and actin cytoskeleton, respectively, in primary HMEC (Figure 2). Based on expression of the targeted red-fluorescent proteins, greater than 90% transduction (delivery) efficiencies were routinely attained in primary HMEC. A validated protocol for BacMam transduction of primary HMEC can be found at **www.invitrogen.com/mammarycells**.

Organelle Lights™ and Cellular Lights™ reagents are ideal for studies of dynamic cellular processes that require accurate and selective labeling of subcellular compartments and structures, including time-lapse fluorescence microscopy and high-content screening. Invitrogen offers an expanding array of probes that take advantage of the BacMam delivery technology, including ion channels, ion sensors, and targeted fluorescent proteins (Organelle Lights™ and Cellular Lights™ reagents), as well as custom services.

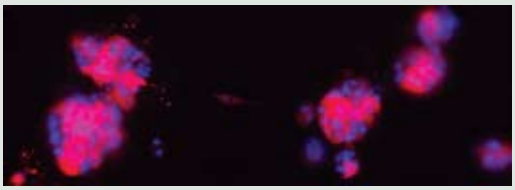

Figure 3—Fixed-cell image of primary human mammary epithelial cells transduced with Cellular Lights™ Actin-RFP and then grown in 3D culture using Geltrex™ Reduced Growth Factor Basement Membrane Matrix. In this fluorescent micrograph (100x magnification), intracellular actin is labeled with Cellular Lights™ Actin-RFP (Cat. no. C10127) and fluoresces red; nuclei are counterstained with the blue-fluorescent Hoechst 33342 dye.

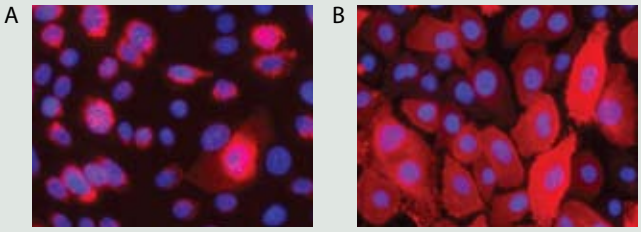

Figure 2—Fixed-cell images of primary human mammary epithelial cells transduced with Organelle Lights™ Golgi-RFP or Cellular Lights™ Actin-RFP. In these fluorescent micrographs (200x magnification), the Golgi apparatus is stained with Organelle Lights™ Golgi-RFP (Cat. no. O10098) and fluoresces red (**A**), or intracellular actin is labeled with Cellular Lights™ Actin-RFP (Cat. no. C10127) and fluoresces red (**B**); in both images, nuclei are counterstained with the blue-fluorescent Hoechst 33342 dye.

Grow transduced HMEC in 3D culture

A significant advantage of the BacMam delivery system is the lack of microscopically observable cytopathic effects in a variety of normal human primary cells following transduction. We have transduced primary HMEC growing in standard 2D culture conditions with Organelle Lights™ and Cellular Lights™ reagents, and then transferred the cells to 3D culture using Geltrex™ Reduced Growth Factor Basement Membrane Matrix. The transduced HMEC expressing the autofluorescent fusion proteins formed acinar structures that were indistinguishable from those of untransduced cells (Figure 3). Furthermore, we used BacMam-mediated transduction followed by cryopreservation on a variety of human cell types without loss of cell viability upon thaw (data not shown). Taken together, these results illustrate that using normal human primary cells in conjunction with BacMam delivery technology provides an extremely efficient system for generating physiologically relevant mammalian cell models. To learn more, visit **www.invitrogen.com/bp58**. ■

References

1. Kenny, P.A. et al. (2007) *Mol Oncol* 1:84–96.
2. Martin, K.J. et al. (2008) *PloS ONE* 3:e2994.
3. Lee, G.Y. et al. (2007) *Nat Methods* 4:359–365.

Product	Quantity	Cat. no.
GIBCO® Human Mammary Epithelial Cells (HMEC)	>500,000 viable cells	A10565
Medium 171	500 ml	M-171-500
Medium 171PRF (phenol red free)	500 ml	M-171PRF-500
Mammary Epithelial Growth Supplement	5 ml	S-015-5
HuMEC Ready Medium (1X), liquid	500 ml	12752010
Geltrex™ Reduced Growth Factor Basement Membrane Matrix	1 ml 5 ml	12760-013 12760-021
Organelle Lights™ Golgi-RFP	1 kit	O10098
Cellular Lights™ Actin-RFP	1 kit	C10127

Hassle-free western blots

THE WESTERNDOT™ 625 WESTERN BLOT KITS.

Avoid X-ray film, developing reagents, and HRP optimization

The new WesternDot™ 625 kits provide low-picogram sensitivity while eliminating the hassle of using a darkroom and developing reagents, or optimizing film exposures. While chemiluminescence is still recommended when the absolute highest sensitivity is required, WesternDot™ 625 kits can greatly simplify your day-to-day protein analysis workflow. The protocol is very similar to standard ECL™ (GE Healthcare) workflows, but uses a biotinylated secondary antibody followed by a Qdot® 625 streptavidin conjugate for detection (Figure 1). No specialized equipment is required—simply use a standard UV light box with an ethidium bromide filter to detect the fluorescent signal. Each WesternDot™ 625 kit contains everything required for detection, including ready-to-use reagents optimized for use on nitrocellulose, PVDF, or nylon membranes, and two staining dishes for standard mini blots.

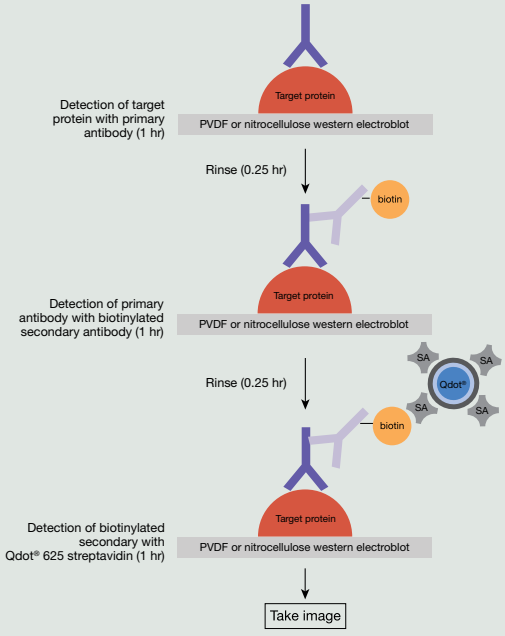

Figure 1—The WesternDot™ 625 kit workflow. The protocol steps and execution times of the WesternDot™ 625 kit are very similar to those of typical ECL™ protocols. However, WesternDot™ detection is optimized right out of the box, whereas ECL™ blots often require several rounds of detection to optimize film exposure and antibody concentrations.

A single blot plus a single dot equals more information

The streptavidin-based WesternDot™ 625 kits can be used to detect endogenous biotinylated proteins, as long as these proteins do not run concurrent with the protein of interest. The endogenous proteins can serve as loading controls, eliminating the need to strip and reprobe the blot for housekeeping proteins such as GAPDH or α-tubulin (Figure 2). It may be possible to perform both high-sensitivity ECL detection for your specific marker and convenient WesternDot™ 625 detection for the more abundant housekeeping proteins, on the same membrane, without stripping the blot. Come out of the Dark Ages with the WesternDot™ 625 Western Blot Kits. Learn more at **www.invitrogen.com/bp58**. ■

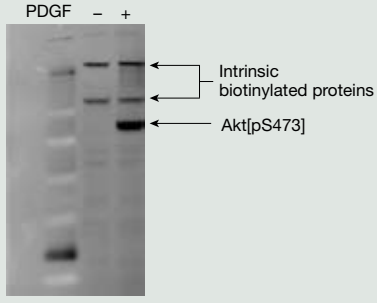

Figure 2—Simultaneous detection of internal controls with phospho-Akt. Extracts of NIH 3T3 cells, either unstimulated (–PDGF) or stimulated with 50 ng/ml PDGF for 15 min (+PDGF), were resolved by SDS PAGE on 4–12% gels and transferred to PVDF with the iBlot® system. The membranes were probed for phospho-Akt with a rabbit monoclonal anti-Akt[pS473] antibody (Cat. no. 44-621G) and detected using the WesternDot™ 625 Anti-Rabbit Western Blot Kit.

Product	Quantity	Cat. no.
WesternDot™ 625 Goat Anti-Mouse IgG Western Blot Kit	20 minigel blots	W10132
WesternDot™ 625 Goat Anti-Rabbit IgG Western Blot Kit	20 minigel blots	W10142

NUCLEIC ACID DEAD CELL STAIN

SYTOX® AADvanced™ dead cell stain is a high-affinity nucleic acid stain for dead cell detection and cell cycle analysis in flow cytometry using the 488 nm blue laser. The dye is spectrally similar to 7-AAD, but with rapid uptake kinetics and relatively low CVs. The stain penetrates cells more efficiently than 7-AAD, providing better separation of live and dead cells. When paired with RNase treatment, SYTOX® AADvanced™ stain can be used for DNA content analysis in fixed cells. Learn more at **www.invitrogen.com/bp58**.

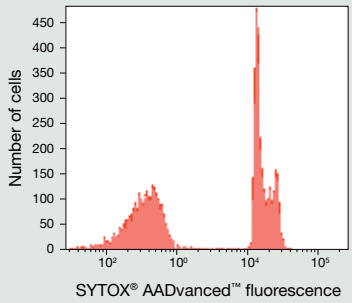

Dead cell discrimination using the SYTOX® AADvanced™ Dead Cell Stain Kit. A mixture of heat-killed and untreated Jurkat cells was stained with SYTOX® AADvanced™ dead cell stain solution for 5 min. Cells were analyzed on a flow cytometer equipped with a 488 nm laser and a 695/40 nm bandpass filter. Live cells are easily distinguished from the dead cell population.

Product	Quantity	Cat. no.
SYTOX® AADvanced™ Dead Cell Stain Kit	500 tests	S10274
SYTOX® AADvanced™ Dead Cell Stain Kit	100 tests	S10349

MOUSE ANTIBODY CAPTURE KIT FOR FLOW CYTOMETRY

The AbC™ Anti-Mouse Bead Kit provides an accurate, easy-to-use technique for setting compensation, and is designed for use with all isotypes of mouse immunoglobulin. The kit provides polystyrene microspheres coated with immunoglobulin (positive compensation beads) and uncoated (negative compensation beads). When mixed with a fluorophore-conjugated mouse antibody, the two bead components provide distinct positive and negative populations for use in setting compensation. This kit demonstrates higher and more consistent reactivity to different subclasses of immunoglobulins than other available controls. Learn more at **www.invitrogen.com/bp58**.

Product	Quantity	Cat. no.
AbC™ Anti-Mouse Bead Kit	100 tests	A10344

STAINS FOR CELL CYCLE ANALYSIS

Vybrant® DyeCycle™ Ruby stain allows cell cycle analysis in live cells by flow cytometry using common 635 nm red laser excitation. The dye emits at >670 nm, placing cell cycle studies within reach of nearly all flow cytometrists while leaving the blue laser channels open for other studies. Compared to DRAQ5, Vybrant® DyeCycle™ Ruby stain provides a low level of toxicity, allowing cells to be analyzed using red laser excitation, sorted, and then regrown. Learn more at **www.invitrogen.com/bp58**.

Product	Quantity	Cat. no.
Vybrant® DyeCycle™ Ruby stain	400 µl	V10273
Vybrant® DyeCycle™ Ruby stain	100 µl	V10309

CYTOKINE RAT 10-PLEX PANEL USING XMAP® TECHNOLOGY

The Cytokine Rat 10-Plex Panel, a multiplex bead-based immunoassay, allows the simultaneous measurement of ten cytokines: IL-1α, IL-1β, IL-2, IL-4, IL-6, GM-CSF, TNF-α, IL-10, IFN-γ, and IL-12. Samples may include rat serum, EDTA, citrate or heparin plasma, or cell culture supernatant. For a complete list of multiplex Luminex® assays, visit **www.invitrogen.com/bp58**.

Luminex® and xMAP® are registered trademarks of Luminex® Corporation.

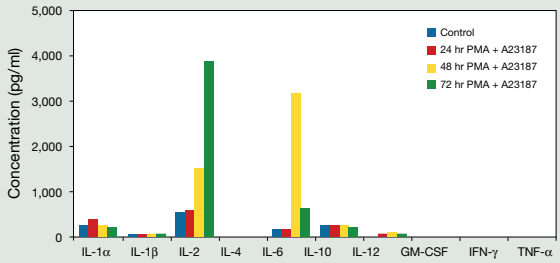

Cytokine production profile of a rat splenocyte detected by the Cytokine Rat 10-Plex Panel. A rat splenocyte was stimulated with 50 ng/ml PMA and 250 ng/ml calcium ionophore (Cat. no. A23187) at 24 hr, 48 hr, and 72 hr. The supernatant was collected and used in a multiplex bead assay.

Product	Species	Quantity	Cat. no.
Cytokine Rat 10-Plex Panel	Rat	100 tests	LRC0002

RESEARCH ANTIBODIES AND ASSAYS

Many new research antibodies and assays are released each month. For a complete list of products validated for western blotting, immunofluorescence, flow cytometry, and more, visit **www.invitrogen.com/bp58**.

Recently published

A LOOK AT HOW YOUR FELLOW RESEARCHERS ARE USING INVITROGEN™ PRODUCTS.

Glycoproteomics: Identification of *O*-GlcNAc modifications in *Xenopus* oocytes. *Xenopus laevis* oocytes exhibit low levels of *O*-linked N-acetylglucosamine (*O*-GlcNAc) protein modification that are insufficient for isolation by immunoprecipitation or WGA lectin affinity capture. For their investigations of cell cycle dependence of *O*-GlcNAc modification in *Xenopus* oocytes, Dehennaut and coworkers therefore turned to the Click-iT® *O*-GlcNAc Enzymatic Labeling System to ligate azide tags to *O*-GlcNAc residues, followed by selective biotinylation of the azide tags using the Click-iT® Biotin Protein Analysis Detection Kit. Proteins were then captured on avidin beads, separated by SDS-PAGE and identified by mass spectrometry. *O*-GlcNAc-modified proteins were identified including cytoskeletal proteins, glycolytic enzymes, regulatory proteins such as protein phosphatase PP2A, and proteins involved in mRNA translation.

Dehennaut, V., Slomianny, M.C., Page, A., Vercoutter-Edouart, A.S., Jessus, C., Michalski, J.C., Vilain, J.P., Bodart, J.F., Lefebvre, T. (2008) Identification of structural and functional *O*-linked N-acetylglucosamine-bearing proteins in *Xenopus laevis* oocyte. *Mol Cell Proteomics* 7:2229–2245.

High-content screening: Multiparametric assessment of hepatotoxicity potential. Mechanistic information derived from image-based high-content screening (HCS) assays offers the prospect of better understanding and predictivity of human hepatotoxicity, thereby alleviating a major drug safety liability. Researchers from Abbott Laboratories report the validation and implementation of an HCS cytotoxicity assay based on simultaneous measurement of eight cell health indicators associated with nuclear morphology, plasma membrane integrity, mitochondrial function, and cell proliferation. This multiparametric readout was derived from image analysis of HepG2 cells stained with Hoechst 33342, tetramethylrhodamine ethyl ester (TMRE), and YOYO®-1. Inhibition of cell proliferation was found to be the most consistently sensitive cell health indicator in the HCS assay. IC_{50} values for test compounds known to have diverse mechanisms of toxicity obtained using the HCS assay were found to be highly correlated with those obtained using the CyQUANT® NF Cell Proliferation Assay. The CyQUANT® NF Cell Proliferation Assay performed with HepG2 cells can therefore be used as an initial screen to accelerate compound prioritization in conjunction with the more comprehensive but time-consuming multiparametric HCS assay.

Abraham, V.C., Towne, D.L., Waring, J.F., Warrior, U., Burns, D.J. (2008) Application of a high-content multiparameter cytotoxicity assay to prioritize compounds based on toxicity potential in humans. *J Biomol Screen* 13:527–537.

Neuroscience: Time-lapse imaging of neuroprotective cellular interactions. A team of Swiss and German researchers reports that ischemic neurotoxicity caused by external application of polymorphonuclear neutrophils (PMNs) in rat brain slices is counteracted by additional application of microglia. Primary rat microglia cultures were prepared using Alexa Fluor® 568 dye–labeled *Griffonia simplicifolia* isolectin (GS-IB4) for assessment of purity. Direct application of microglia to organotypic hippocampal slice cultures (OHCs) resulted in a significant reduction of PMN-evoked neuronal damage visualized using propidium iodide. The implication of direct interactions between microglia and PMNs was then explored using time-lapse confocal and two-photon excitation microscopy using CellTracker™ Green CMFDA, CellTracker™ Orange CMTMR, or CellTracker™ Blue CMAC to label microglia and PMNs. Microglia were observed to pursue and then engulf viable, motile, nonapoptotic PMNs in both OHCs and PMN–microglia co-cultures, representing a novel postischemic damage control mechanism that is only detectable by live-cell imaging.

Neumann, J., Sauerzweig, S., Rönicke, R., Gunzer, F., Dinkel, K., Ullrich, O., Gunzer, M., Reymann, K.G. (2008) Microglia cells protect neurons by direct engulfment of invading neutrophil granulocytes: a new mechanism of CNS immune privilege. *J Neurosci* 28:5965–5975.

Protein structure/function: The molecular basis of pH-dependent penicillin susceptibility of MRSA. Why are methicillin-resistant *Staphylococcus aureus* (MRSA) pathogens susceptible to β-lactam antibiotics at pH 5 but not at pH 7? In pursuit of answers to this question, Lemaire and coworkers used BOCILLIN™ FL penicillin to measure penicillin binding to MRSA cultures and to purified penicillin-binding protein 2a (PBP 2a). PBP 2a is a crosslinking transpeptidase that has been identified as the principal MRSA resistance factor for β-lactam antibiotics. BOCILLIN™ FL penicillin binding to MRSA and to PBP 2a was found to increase ~50-fold and ~5-fold, respectively, at pH 5.5 and pH 7. Together with circular dichroism spectroscopy and enzyme kinetic data, the BOCILLIN™ FL penicillin binding measurements indicate that acidic pH causes a significant change in the conformational properties of PBP 2a, rendering it more susceptible to inhibitory acylation by β-lactams and offering a prospective novel point of intervention for MRSA antibiotic therapy.

Lemaire, S., Fuda, C., Van Bambeke, F., Tulkens, P.M., Mobashery, S. (2008) Restoration of susceptibility of methicillin-resistant *Staphylococcus aureus* to β-lactam antibiotics by acidic pH: role of penicillin-binding protein PBP 2a. *J Biol Chem* 283:12769–12776.

The publications summarized here are just a few of the recent additions to the 59,000+ references describing applications of Invitrogen™ products in our searchable bibliography database. Visit www.invitrogen.com/support to search for citations by product.

WANT TO SEE YOUR NAME ON THIS PAGE?
Send your bibliographic references featuring Invitrogen™ products to bioprobes@invitrogen.com.